Assessment of soil physical properties and shallow groundwater recharge in the Ashanti region of Ghana

Johannes Herzog

Master of Science Msc. • 30 credits
Swedish University of Agricultural Sciences, SLU
Department of Soil and Environment
Environmental Sciences in Europe (EnvEuro)
Examensarbeten/Institutionen för mark och miljö, SLU
Part number 2024:15
Uppsala 2024

Assessment of soil physical properties and shallow groundwater recharge in the Ashanti region of Ghana

Johannes Herzog

Supervisor:	**Jennie Barron, Swedish University of Agricultural Science, Department of Soil and Environment**
Assistant supervisor:	Seifu Tilahun, International Water Management Institute (IWMI)
Assistant supervisor:	Michael Stockinger, University of Natural Resources and Life Sciences (BOKU), Department of Water, Atmosphere and Environment, Institute of Soil Physics and Rural Water Management
Examiner:	Nicholas Jarvis, Swedish University of Agricultural Science, Department of Soil and Environment

Credits:	30 credits
Level:	A2E
Course title:	Master Thesis in Environmental science
Course code:	EX0897
Programme/education:	EnvEuro - Environmental Science – Soil, Water and Biodiversity
Place of publication:	Uppsala, Sweden
Year of publication:	2024
Copyright:	All featured images are used with permission from the copyright owner.
Keywords:	tropics, cocoa, agricultural management, groundwater recharge

Swedish University of Agricultural Sciences
Department of Soil and Environment

Abstract

This study projected shallow groundwater recharge processes in the sub-humid, agroforestry dominated Mankran watershed based on assessment of soil physical properties and application of the Chloride Mass Balance (CMB) and Water Table Fluctuation (WTF) methods. The objective was to enhance understanding of groundwater recharge in a tropical, cocoa forest dominated landscape with diverse land use and soil properties. Soil samples from 0 – 40 cm were analysed for texture, pH, organic matter content and bulk density. Additionally, topsoil field-saturated hydraulic conductivity (Kfs) was measured with single ring infiltrometers. The results revealed significant spatial variability with high sand contents ranging from ca. 60 – 80 % and near-neutral pH associated with higher infiltration rates, particularly in cocoa fields (120 – 200 mm h^{-1}). During the study period of June 2023 – July 2024, shallow groundwater recharge rates estimated by the CMB method ranged from ca. 12 – 34 % (144 – 408 mm) of about 1200 mm rainfall, whereas the WTF method often produced higher and potentially overestimated rates. The findings pointed out the complexity of groundwater recharge processes and the necessity of applying multiple estimation methods for accurate assessment. Despite limitations in soil sampling and method applicability, the study provided valuable data enlarging sparse soil data basis while simultaneously giving insights into the hydrological dynamics of the Mankran watershed. These insights promote more informed, sustainable land use and agricultural management practices in the region, highlighting the importance of comprehensive soil and water data collection.

Keywords: tropics, cocoa, agricultural management, groundwater recharge

Table of contents

List of tables

List of figures

INTRODUCTION

In the last decade, population in Western and Central Africa increased by almost 30% (FAO, 2022). Global conflicts and challenges such as the war in Ukraine and COVID 19 further aggravated current poor economic development and together with climate change, pressure on agricultural productivity for guaranteeing food security rose (Enahoro et al., 2023). Consequently, land use changes, converting natural forest in humid and sub-humid tropical catchments into productive agricultural land, took place. Climate change has already led to unpredictable weather patterns. The ongoing shift of Ghana's seasonal precipitation patterns poses a threat to rain fed agriculture (Ministry of Food and Agriculture, 2024). Possible impacts on underlying shallow groundwater resources and the operating space of its outtake for irrigation purposes are to date less well understood. Yet, these regions hold a great potential for agricultural intensification to contribute both: food, nutrition and income whilst ensuring sustainable land use (Tilahun et al., 2023).

In this work, assessment of top soil physical properties aimed to enhance understanding of ongoing shallow groundwater recharge processes paving the way for suitable agricultural management practices. The study area encompassed the Mankran micro watershed located in the Ashanti region of Ghana where cocoa forests dominated the upper parts and illegal small scale mining activities cut through the landscape in the lower parts. Analysis of groundwater recharge did not only quantify renewable groundwater resources but simultaneously assessed the vulnerability to contamination or drought. Furthermore, potential impacts of land use changes and climate on water resources were represented. Many methods estimate groundwater recharge, all showing strengths and weaknesses, potentially leading to different results. For a representative estimation, it was therefore recommended to use multiple methods (Healy, 2010). The methods used in this study were the Water Table Fluctuation Method (WTF) and Chloride Mass Balance (CMB). Both but especially CMB served as suitable tool for recharge estimations in different parts of Ghana (Akurugu et al., 2019; Boansi Okofo et al., 2022; Duah et al., 2021; Manu et al., 2023; Obuobie et al., 2012; Zango et al., 2023). The following research questions aimed not only to outline possible seasonal recharge scenarios but examine the relation between topsoil physical properties and shallow groundwater recharge processes in the study area:

1) How can collected, local soil data better inform estimations of underlying groundwater recharge?

2) What spatial and temporal variations in shallow groundwater recharge rates in the Mankran watershed of Ghana can be estimated by the Chloride Mass Balance (CMB)?

3) Is the level of shallow groundwater recharge calculated with the Water Table Fluctuation (WTF) approach comparable to the results obtained by the CMB?

1. BACKGROUND

1.1 Approaches to estimate groundwater recharge

Applied methodologies to estimate water quantities in Ghana were commonly based on remote sensing techniques and surface water balances (Dekongmen et al., 2022; Ofosu et al., 2014). Thus, collected ground data was seldom the basis for estimated results. Besides sparse applications of the WTF method, broadly used methods to estimate groundwater recharge were based on the presence of multi environmental tracers such as stable isotopes of water ($\delta^{18}O$ and $\delta^{2}H$), sulphur hexafluoride (SF6), chlorofluorocarbons (CFCs) or chloride in rain, surface – and groundwater (Akurugu et al., 2019; Boansi Okofo et al., 2022; Gibrilla et al., 2022; Zango et al., 2023).

The tracer method, namely Chloride Mass Balance (CMB), and the Water Table Fluctuation method (WTF) were the main approaches used for describing groundwater recharge in this work. Not least since they were demanding simpler data collection and inputs than others, like the soil moisture – or water balance method. The WTF computed recharge from rising and falling water tables in observation wells assuming a dependency on percolated rainfall. With additional knowledge about the water yielding characteristics of the soil, recharge was estimated over time (Healy & Cook, 2002). In case of spatially far distributed groundwater wells showing highly varying recharge rates, averaging an overall recharge for a bigger area could be difficult (Abera Beyene et al., 2019). The CMB used chloride fractions in rain, surface- and groundwater estimating recharge numbers through tracing concentrations (Guan et al., 2009). The reliability of the CMB was tied to some assumptions e.g., regarding chloride sources and depends on the amount of conducted measurements. Estimations, however, should be applicable on a bigger spatial scale than results from the WTF method. Latter could give higher but supposedly more accurate point recharge numbers whereas trust in CMB delivering representative results despite assumptions was generally high (Walker et al., 2019).

1.2 Groundwater recharge in Ghana

With most studies conducted in the Volta region and northern Ghana, the Ashanti region has seldom been targeted for groundwater estimation studies. However, there were similar natural conditions like average rainfall rates and geologic conditions found between conducted research in other areas and the study area in the Ahafo Ano South district at the centre of this work. Comparison to ground water recharge estimations and characteristics found in other studies should therefore help to validate the tendency calculated with the Chloride Mass Balance (CMB).

According to the presence of stable isotopes δ^2H and $\delta^{18}O$ in the rain, the surface- and groundwater, recharge in the Volta region happened during the raining season, from June until August. The average recharge amount was estimated between around 80 and 85 mm per month. Detected limitations included lack in reliable rain data and the need for more monitored tracers. Both would increase the trust in obtained results (Gibrilla et al., 2022). Another study in the upper east region not only used δ^2H and $\delta^{18}O$ but also chloride as tracer method to estimate the recharge. The rates were around 20 mm per year or about 2 % of 1000 mm yearly rainfall. However, as major constraint chloride was suggested to be of meteoric origin affecting the applicability of the CMB (Akurugu et al., 2019). The wide range of results that the Chloride Mass Balance delivered in this area was confirmed by (Boansi Okofo et al., 2022). They estimated the recharge in the area from 0.2 to 24.8 % with an average of 7 % of the annual precipitation. In contrary to Akurugu et al., 2019, the presence of chloride was linked to its introduction into the water cycle through precipitation. Similar methods as before came to the conclusion that the annual groundwater recharge in the Upper East region could be expected between around 2 and 13.5 %. While narrowing down the previously mentioned ranges, Zango et al., 2023 presented a similar average of about 5 % of the mean annual rainfall. The lower part of the Volta Basin, the Afram Plains, was characterised by a SWAT simulated mean annual rainfall of about 1200 mm with 30 % or about 400 mm recharged to the shallower and deeper groundwater aquifers. Those averages based on significant spatial differences within the Afram Plains reaching from 0 – 100 mm recharge per year (Dekongmen et al., 2022). In the Densu Basin, in south eastern Ghana, precipitation varied between 800 and 1700 mm per year. Chloride Mass Balance (CMB) revealed an average of 0.4 to 320 mm with a mean of 70 mm recharged. The application of the Water Table Fluctuation (WTF) method came to a wider range of about 6 – 500 mm yearly recharge into the groundwater body (Duah et al., 2021).

As common in the cited studies above, a relatively wide range of almost 0 – 34 % was estimated in the Pra-River Basin using the Chloride Mass Balance while WTF estimated only 0 – 3.6 % of 1500 mm annual rainfall (Manu et al., 2023). The mentioned studies revealed similar estimations of groundwater recharge in environmentally related parts of Ghana. Consequently, it seemed appropriate to

expect up to 30 % groundwater recharge of the annual precipitation as a benchmark for the Mankran watershed. Limitations were namely: spatial representativeness of estimation values; adverse sources introducing chloride; insufficient collection of data and/or range of methods.

1.3 Soil physical properties related to study area

In order to put gathered field data into perspective, sampled soil physical properties influencing groundwater recharge processes are presented. Texture and permeability, depth of soil profiles, hydraulic conductivity and organic matter content were relevant to understand prevailing water flow through the soil and resulting recharge patterns. That being said, coarse-textured, porous and permeable soils with deep profiles and high organic matter are most conducive to groundwater recharge (National Research Council, 1994). Such properties were known for similar geology and land use types in the surroundings of the study area Figure (1) allowing comparison to later presented results from field work. However, this data from literature was widely limited to the topsoil, often not exceeding 10 cm depth. The following Table (1) displays a data compilation of comparable land use types in 0 – 30 cm with mostly similar texture as expected in the Mankran watershed. All locations were lying on the same bedrock, namely the Birimian Supergroup. Disregarding differences in texture, bulk density was lower at cocoa fields than in former mining areas or plantain fields. However, the compactness does increase up to 1.6 g cm^{-3} in 20 – 40 cm (Mohammed et al., 2016). Soil pH on the other side was much higher and found around neutral for cocoa while other land use types were quite acid. MIR spectroscopy predicted organic matter content at Kubease over 10 % at forest and woodland cover. Cocoa fields ranged up to similar fractions but the other land use types were found in smaller magnitudes of 1 - 5 %. The understanding of hydrological processes in cocoa agroforests is limited (Farrick & Gittens, 2023). That to say, studies collecting data at mining areas were even more difficult to find. Measured saturated hydraulic conductivity values (Kfs) at the other land use types was varying with the highest infiltration rate in the forest at Kubease. Field Capacity (FC) and Wilting point (WP) were subject to varying analysis methods applying different ranges of pressure. For Loamy sand, Sandy loam and Sandy clay loam a global meta study by Gupta et al., 2021 averaged FC at 17.3, 24.2 and 28.7 % and WP at 6.5, 11 and 17.1 % from more than 7,000 measurements. Varieties in applied pressures are therefore expected to be considered.

Table 1. Topsoil data compilation from comparable geographic features as the Mankran watershed. OM = organic matter and Kfs = field-saturated hydraulic conductivity

Sources	Location	Land use type	Texture	Depth (cm)	Bulk density (g cm^{-3})	pH (1:1, water)	OM %	Kfs (mmh^{-1})
Ofori et al., 2013	Biemso	Plantain	Silt loam	0 - 20	1.21 - 1.30	4.2-4.73	1.2-2.95	4.11-23.87
Ofori et al., 2013	Biemso	Fallow land	Silt loam	0 - 20	1.07 - 1.35	4.7-6.45	0.86-4.1	29.30-60.06
Fosu-Mensah et al., 2016, p. 2	Nkrankwanta	Cocoa	Sandy loam	0 - 20	1.10 (Mohanmmed et al., 2016)	7.34-7.80	1.54-3.36	No data
	Diabaa		Sandy clay loam	0 - 20		7.73-7.96	9.78-10.3	No data
Okoh & Zakpaa, 2024	Afiesa	Mining	Loamy silt	15 - 30	1.58	6	0.471	No data
Gupta et al., 2021	Estimates from global data	various	Loamy sand	0 - 20 (assumption by authors)	1.55	No data	1.94	55.14
			Sandy clay loam		1.53	No data	2.17	5.93
			Sandy loam		1.49	No data	2.29	31.07
Bargués-Tobella et al., 2024	Kubease	Forest	Sandy loam	0 - 20	No data	4.85	13.18	58.84
		Woodland	Sandy clay loam			6.28	12.20	9.10

Figure 1. Sites with comparable soil data (blue) in proximity to Mankran watershed (red) and the districts of Ahafo Ano (purple) and Ashanti (green)

2. MATERIALS AND METHODS

2.1 Study area

The Mankran micro watershed (122 km^2) is located in the Ahafo Ano South district (Ashanti region). Forest – cocoa plantation and mining activities along with reclaimed land dominate the upper and lower parts of the area (Adusei-Gyamfi et al., 2023) Figure (2). The topography is undulating from flat to hilly. The area is

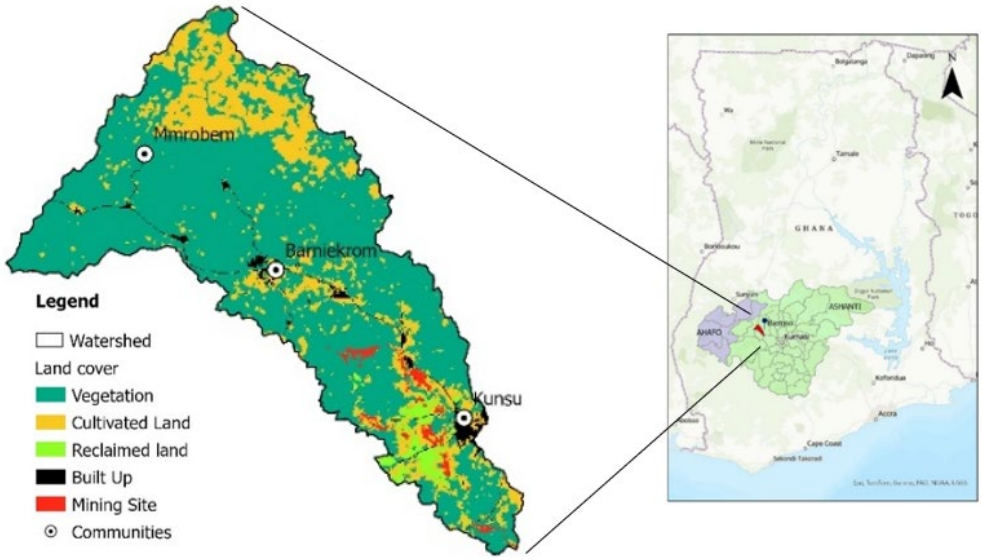

Figure 2. a) Land cover (left) (Copernicus Land Monitoring Service information 2024 under https://dataspace.copernicus.eu/) and b) location of watershed (red) in Ghana (right) (World Topographic Map, ESRI 2024)

dominated by semi-deciduous forest and the mainly drained by the Mankran river. Besides forest, the district is known for its mineral deposits. Granit, bauxite, and manganese are being mined extensively (Anim-Gyampo et al., 2021). Within the Mankran watershed, around Kunsu, illegal gold mining activities are contributing to significant land use change (AASWDA, 2018; Adusei-Gyamfi et al., 2023; Anim-Gyampo et al., 2021). Figure (3) shows the mining activities (surrounded in red) around Kunsu and the southeastern border of the watershed in blue.

Figure 3. Satellite Image of mining around Kunsu (surrounded in red)

Commonly referred to as the major food basket of Ghana, about 80 % of the Ahafo Ano South District is arable land. While all kinds of vegetables and crops are prominent, cultivated cash crops are cocoa and cashew (Anim-Gyampo et al., 2021). The elevation of the Mankran watershed is on average about 284 m ranging from 186 (southeast) to 536 m (northwest) with an average slope of 5.49° or 9.8 % Figure (4).

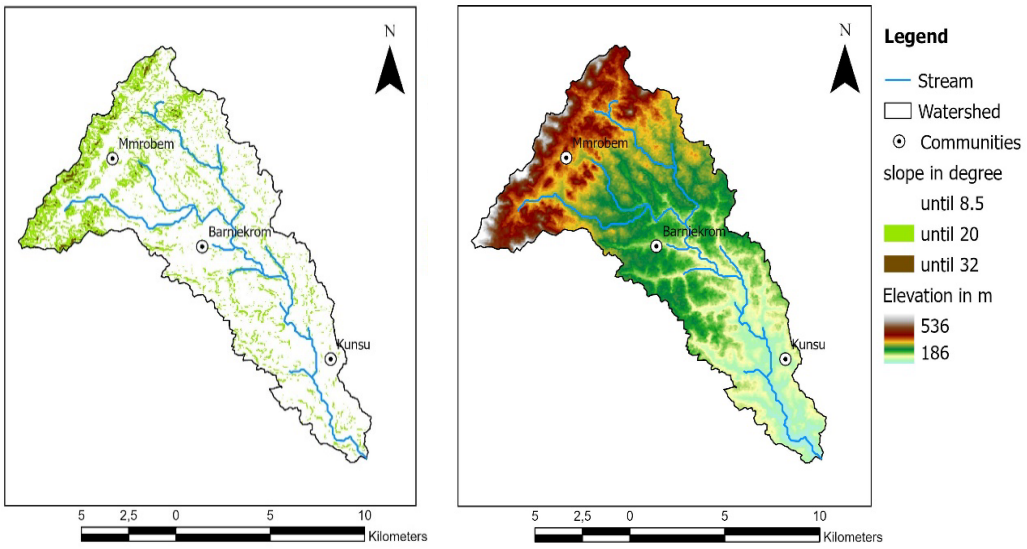

Figure 4. Digital elevation model of Mankran watershed with slope (left) and elevation (right) (after Assefa et al., 2023)

2.2 Climate and water balance

The Mankran watershed, located in Ghana's wet semi-equatorial region, has a bi-modal rainy season: March to July (peaking in May and June) and September to November. Yearly rainfall varies between 1,250 mm in Ahafo and 1,300 mm in

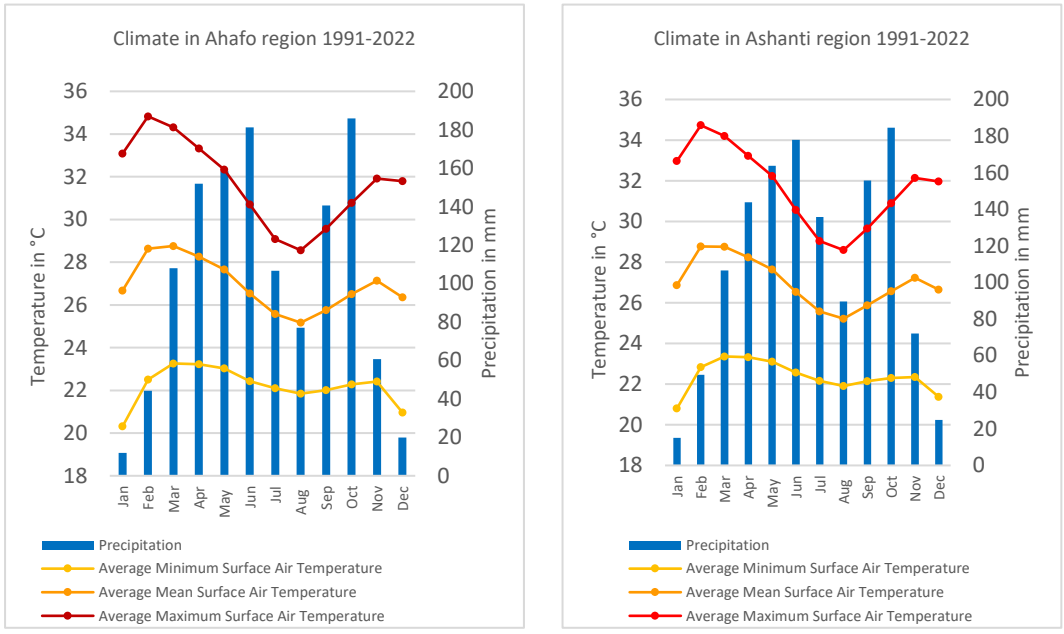

Figure 5. Climates in Ahafo - and Ashanti region (The World Bank Group, 2021)

Ashanti Figures (1) and (5) (The World Bank Group, 2021). Near Biemso Figure (1), the average is around 1,400 mm per year (Baffour et al., 2012).

Rainfall distribution is uneven, with 75 % falling during the major rainy season (Ministry of Food and Agriculture, 2024). In a simple water balance, precipitation (P) equals runoff (R), the sum of potential evapotranspiration (ET) and changes in soil moisture storage (ΔS), like in equation (1) (ICARDA, 2024).

$$P = R + ET + \Delta S \quad (1)$$

Assuming there is no restriction on available water, so called potential evapotranspiration (PET) in the area was dated with around 1,300 mm more than 20 years ago (Christiansen & Awadzi, 2000). Other estimates average PET in the area at about 1,400 mm (Mensah, 2009). The average yearly temperature is 27°C, fluctuating between 22°C and 32°C. The driest months, December to March, often exceed 30°C before the rains. This period features the “Harmattan Winds” bringing dusty air from the Sahara (AASWDA, 2018; Anim-Gyampo et al., 2021; Hastenrath, 1985).

2.3 Geology and soils

The study area is primarily underlain by ancient paleo-proterozoic rocks, including the crystalline Birimian and Tarkwaian groups and the Eburnean Plutonic Suite Figure (6). The Birimian supergroup comprises metamorphosed sediments, tuff, and lava flows, while the Tarkwaian group consists of quartzites, phyllites, grits, and conglomerates with epidorite intrusions. The Eburnean Plutonic Suite includes granitoids like hornblende and biotite granites, granodiorites, and gneiss (Dapaah-Siakwan & Gyau-Boakye, 2000; Gill, 1969; Kesse, 1985). Together, the Birimian

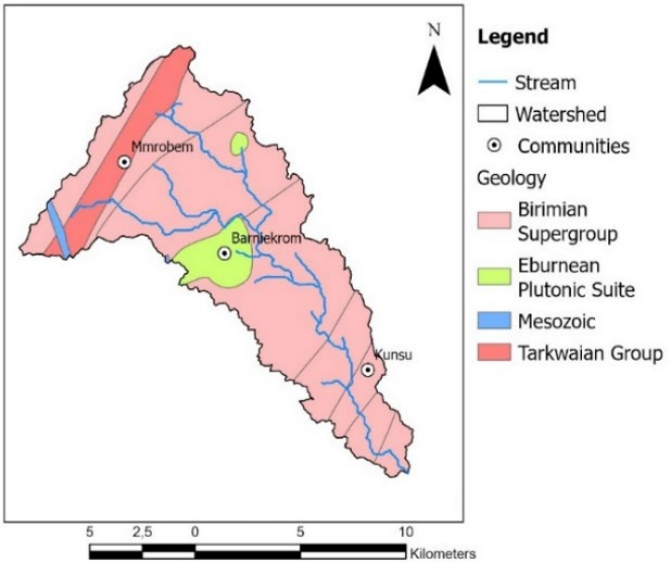

Figure 6. Geology in the study area (Agyei Duodu, 2009)

and Tarkwaian groups dominate almost 80 % of the watershed (62 % and 15 % respectively). About 8 % of the area is of Mesozoic origin (Agyei Duodu, 2009). Groundwater flow and resources in these crystalline rocks are significantly influenced by fractures and joints. Foliation and structural alignment can result in higher water yields in the Tarkwaian and Birimian groups ranging from 30 over 60 l min^{-1} (Appiah-Adjei & Osei-Nuamah, 2017). Within the weathered zone potentially ranging down to 70 m (Asomaning, 1992), the presence of clay is crucial in defining hydrogeological conditions and consequently recharge to groundwater bodies. Low clay contents and thick weathered zones should therefore increase the water flow to wells (Yidana et al., 2015). In the lower Birimian rocks, weathering processes can reduce water storage capacity. Layers at 2 – 3 m below the surface turn soft phyllite and clay into stones and gravel, increasing porosity (Adu, 1992). The Mankran watershed, located in Ghana's semi-deciduous forest zone, primarily features mineral soils shaped by a wet (sub)-tropical climate. The soils in Ahafo Ano South district were classified as Ferric Acrisols, Rhodic Nitisols, and Haplic Alisols, with Acrisols being the most prevalent (Adusei-Gyamfi et al., 2023).

Similar data type expect solely Orthic Acrisols in the Mankran watershed Figure (7).

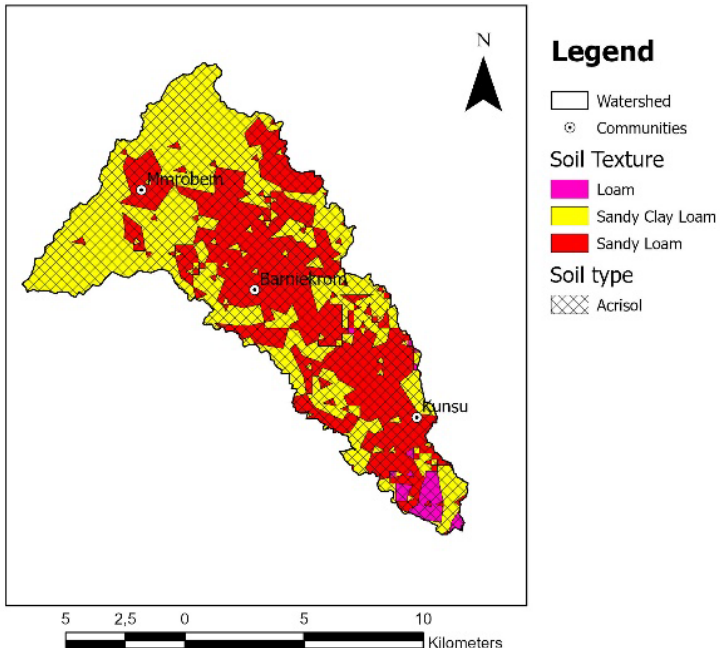

Figure 7. Soil texture and type (Sparks & Hengl 2017)

Orthic Acrisols are acidic, clay-rich, and low in nutrients, often presenting challenges for agriculture due to their aluminum toxicity and erosion risk (Driessen et al., 2001). However, in this region, climate and landscape support Ghanaian Forest Ochrosols, which are red and yellow soils with high organic matter in the topsoil, making them suitable for crops like cocoa, coffee, and oil palm (Effland et al., 2009). Global satellite data suggests that the dominant surface soils in the watershed are Sandy Clay Loam and Sandy Loam Figure (7) (Sparks & Hengl, 2017). This aligns with broader analyses that classify Ghana's cocoa-growing regions similarly (Bationo et al., 2018).

2.4 Data collection and analysis

This thesis examined soil properties in the Mankran watershed through field sampling. Additional, data for the estimation of groundwater recharge was gathered by IWMI-trained citizen scientists starting in June 2023 (Adusei-Gyamfi et al., 2023). Analysis was conducted by KNUST, CSIR - Soil Research Institute, and Thaumasion Consultancy. Maps were created using ArcGIS Pro 3.2, statistical analysis with Minitab 22 and R, calculations in MS Excel 2016. Collected data encompassing texture, bulk density, organic matter and pH was tested on correlations using one way ANOVA analysis with $\alpha = 0.05$ or 0.01 as threshold.

2.4.1 Data collected by citizen scientists (CS)

In three watershed communities, daily rainfall was monitored at 6 am and 6 pm using manual gauges and an automated gauge for calibration (Adusei-Gyamfi et al., 2023). Surface water flow rates at Kunsu and Barniekrom were measured using manual gauges and calculated by timing leaf drops over 10 m Figure (8). Surface runoff was measured using a stage-discharge curve. This, combined with the cross-sectional flow area, determined the flow rate in m^2 s^{-1}. Surface runoff was measured daily and after storms using a stage-discharge curve (Adusei-Gyamfi et al., 2023).

Figure 8. Manual stream gauges at Kunsu (left) and Barniekrom (right)

Since monitoring started on 16th June 2023, hydrological data from the first raining period until December 2023 was incomplete. Similarly, in 2024 data was included until the end of July while the second raining period was missing entirely.

Groundwater levels were measured in the same period, daily in 6 out of 9 wells across the watershed (2 in Kunsu; 3 in Barniekrom and 1 in Mmrobem). AC clamp meters were roped down by the CS until a voltmeter detected current flow indicating reach of the water level. At Kunsu and Barniekrom, two Heron Skinny Dippers were sent done twice a week in similar manner for calibration purposes (Adusei-Gyamfi et al., 2023).

Figure (9) shows all measuring stations: Observation wells (MGW, BGW, KGW), rain gauges (MrainG, BrainG, KrainG), and streamflow gauges (MSW, BSW, KSW) at Mmrobem, Barniekrom, and Kunsu. Qualitative parameters in rainwater, surface water and observation wells were part of the monitoring program and taken on a monthly basis. For this work, solely Cl^- concentrations are relevant as basis for the application of the CMB method.

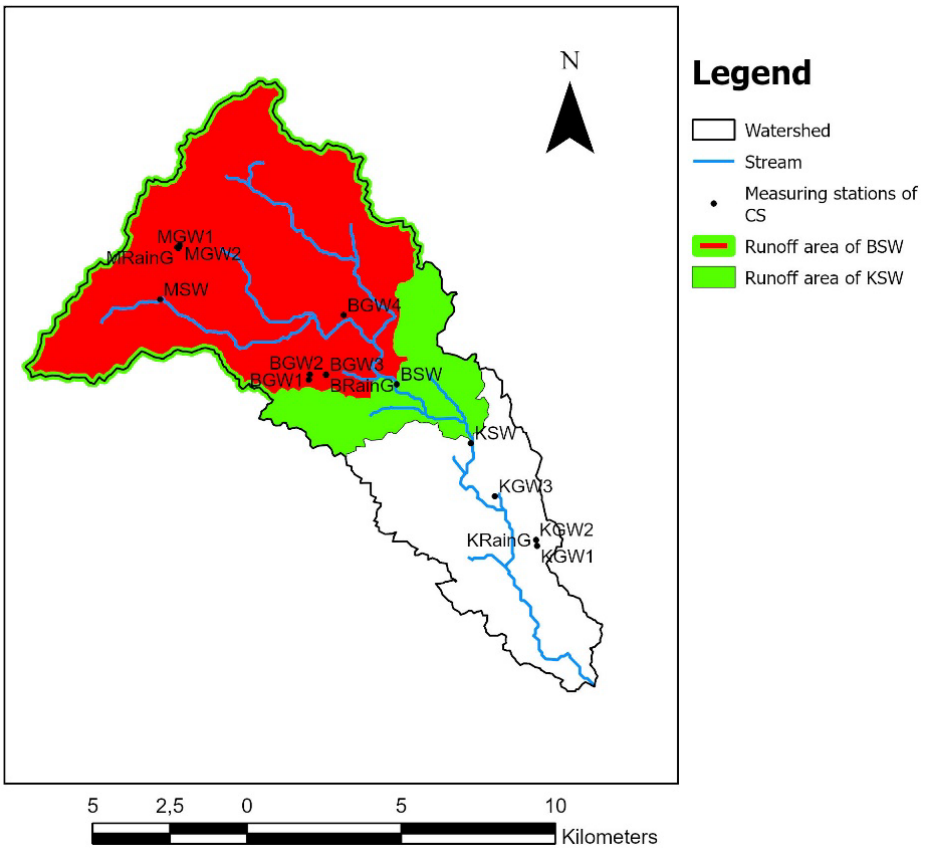

Figure 9. Stations and runoff areas with ongoing measurements by citizen scientists (CS)

2.5 Soil sampling strategy and analysis

For applying the WTF method, soil properties (bulk density, texture, and field capacity) were measured near groundwater observation wells. Zone sampling, combined with topographic/geographic unit sampling, was used to minimize sample numbers and determine locations (Austin et al., 2020; Vågen et al., 2020). To address potential variability related to land use and watershed position, measurement points were selected based on different management practices and positions (upstream/downstream) (Dinkins & Jones, 2008). Sampling considered land use (agroforest, agriculture, mining) and elevation: Kunsu (186 – 250 m, mining), Barniekrom (250 – 300 m, agriculture), and Mmrobem (300 – 536 m, agroforest) Figure (10) (Adusei-Gyamfi et al., 2023). Each community cluster represented various land uses and locations, resulting in nine measurement subplots.

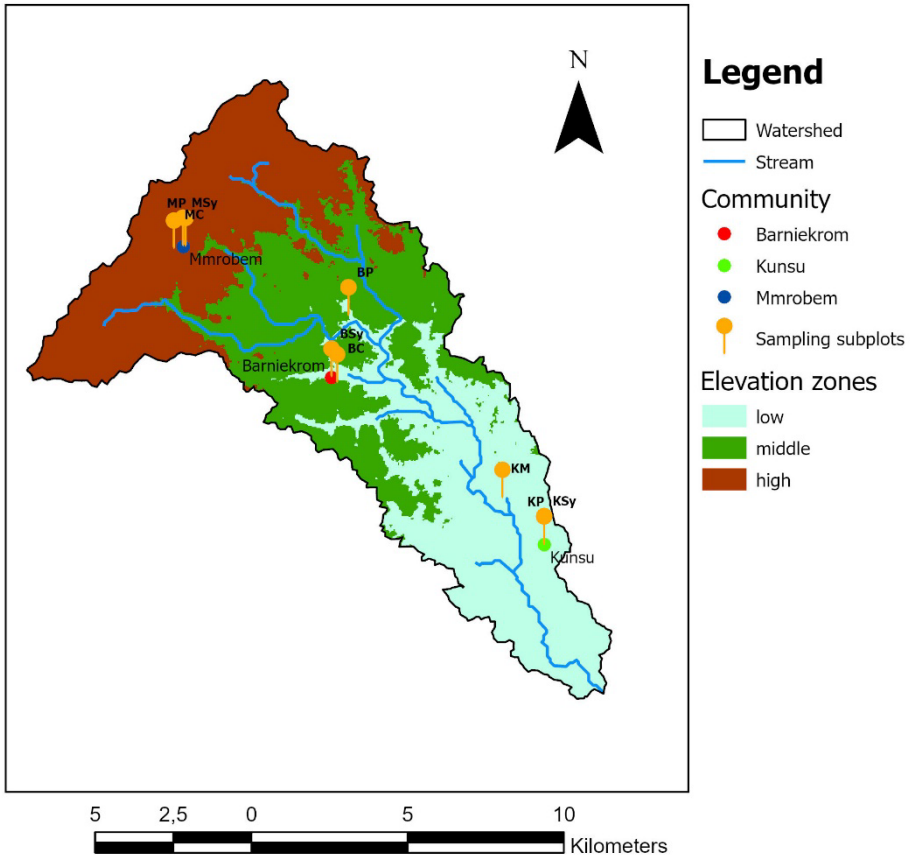

Figure 10. Elevation zones with sampling subplots

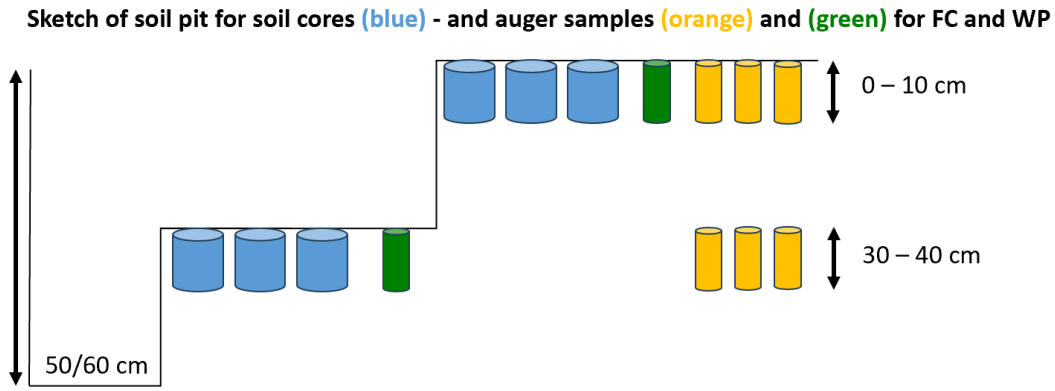

Figure 11. Sampling performance strategy

Soil samples were taken at 0 - 10 cm and 30 - 40 cm depths using a metal core and soil auger Figure (11), adhering to the Land Degradation Surveillance Framework (LDSF) guidelines (Vågen et al., 2020). Compacted, dry soil and big gravel stones jeopardized the equipment provoking adaption of sampling amounts and desired depths at some subplots Table (2).

Table 2. Compilation of all taken samples

	Built-up (next to wells)	**Plantain**	**Cocoa (mid – and upstream)**	**Mining (downstream)**	**Total**
Downstream/mining (Kunsu)	**8*** in 0-10 1 in 10-20 **2*** in 20-30 **	6 in 0-10 1 in 10-20 3 in 30-40 **	No cocoa in area	6 in 0-10 3 in 10-20 **	30
Midstream/agriculture (Barniekrom)	**7*** for 0-10 **7*** for 30-40	6 in 0-10 1 in 10-20 6 in 30-40	6 in 0-10 1 in 10-20 6 in 30-40	No mining in area	40
Upstream/agroforest (Mmrobem)	**7*** for 0-10 **8*** for 30-40	6 in 0-10 1 in 10-20 6 in 30-40	6 in 0-10 1 in 10-20 5 in 30-40 **	No mining in area	40
***next to wells at least one more for FC and WP**					**110**
**** adapted sampling due to constraints**					

Bulk density and gravimetric soil moisture were measured by drying and weighing samples. Composite loose samples determined soil texture, field capacity, and wilting point Figure (12).

Figure 12. From left to right: Soil auger, taking of composite samples and drying of composite samples

Soil texture was classified after the USDA soil texture triangle. Additional soil properties like pH and organic matter were analysed by the laboratory of environmental sciences at KNUST. Texture was identified after drying with the hydrometer method (Page, 1982) and pressure plate analysis delivered field capacity at 0.33 bar and wilting point at 15 bar Appendix (1) (Abbott, 1987; McIntyre, 1974).

2.5.1 Topsoil field-saturated hydraulic conductivity (Kfs)

Kfs was measured at all subplots except the abandoned mining site to understand topsoil infiltration. 200 mm long PVC pipes with a diameter of 105 mm were used as single ring infiltrometers following the LDSF guidelines (Bargués-Tobella et al., 2024). After inserting the device into the soil, water was added, and the drop in water level was recorded at intervals of 5, 10, and 20 min, continuing for up to 160 min Figure (13). Kfs for each tube was then calculated from their last three

Figure 13. PVC ring infiltrometers performing infiltration methods in the field

stabilized infiltration rates by using the method of Nimmo et al., 2009 with equations from D. Reynolds et al., 2002 and W. D. Reynolds & Elrick, 1990.

2.6 Chloride Mass Balance (CMB)

The Chloride Mass Balance (CMB) method relies on the concentration of atmospheric chloride in precipitation and dry deposition accumulating in soil water via evapotranspiration (Guan et al., 2009). This method applies to both unsaturated and saturated zones using chloride levels in soil or groundwater (Somaratne & Smettem, 2013). In this study, the CMB was used in the saturated zone, namely groundwater tables 2 - 13 m below the ground, requiring chloride levels in precipitation, surface water, groundwater and average precipitation values all collected by the citizen scientist (CS). The CMB can be scaled spatially and temporally (Walker et al., 2019). Several assumptions underpin its use: all groundwater chloride originates from precipitation, chloride behaves conservatively without degradation, groundwater evaporation does not occur before sampling, and there is no ongoing chloride recycling. Additionally, chloride concentration in precipitation and precipitation rates must remain steady over time (Bazuhair & Wood, 1996). Figure (14) is schematically representing the assumed chloride concentration flow paths. Evapotranspiration increases chloride concentrations but does not move it.

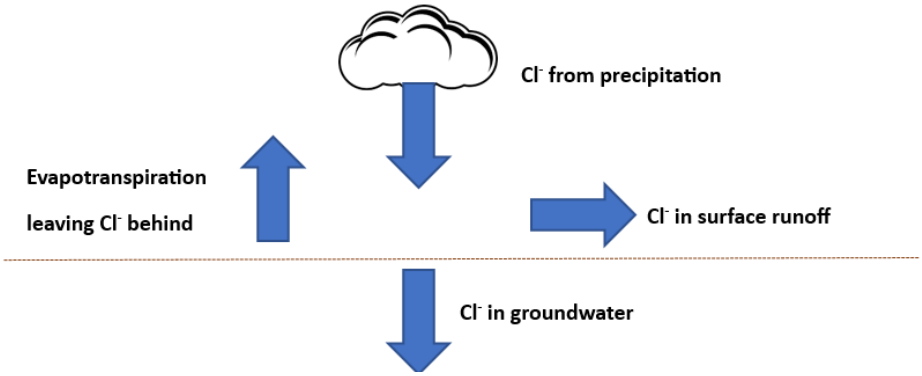

Figure 14. Schematic chloride pathway

While evaporation being an essential parameter within a water balance, quantification is not relevant for application of the CMB (Meinzer, 1923). For actual application, known chloride mass flows are assumed to be in balance as in equation (2).

$$P_{eff} * Cl_{wap} = R_{gw} * Cl_{gw} + \Delta s \quad (2)$$

Where P_{eff} marks the effective precipitation or rainfall minus runoff (mm), Cl_{wap} representing the weighted average chloride concentration in the precipitation including dry deposition, R_{gw} accounting for the recharge (mm) and Cl_{gw} for

chloride concentration in the groundwater (all in mg L^{-1}). To fulfil the steady state assumption, change in storage of chloride in the soil (Δs) is assumed to be zero. Actual groundwater recharge can then be estimated through rearranging (2) as in equation (3) (Walker et al., 2019):

$$R_{gw} = \frac{P_{eff} * Cl_{wap}}{Cl_{gw}} \quad (3)$$

In order to facilitate calculation with known runoff processes in the watershed, the following adapted version (4)was used to calculate the recharge on a seasonal level:

$$R_{gw} = \frac{(P * Cl_p) - (R_s * Cl_s)}{Cl_{gw}} \quad (4)$$

With again R accounting for the recharge (mm), P the measured precipitation (mm), Cl_p, Cl_s and Cl_{gw} as the chloride concentrations in precipitation, surface – and groundwater (all mg L^{-1}) respectively. And R_s representing the surface runoff (mm). All values are from observations taken by the citizen scientists.

2.7 Water Table Fluctuation (WTF)

This method assumes that recharge in unconfined aquifers is solely due to rainwater reaching the water table. It is ideal for shallow groundwater with significant level changes and depends on the number and representativeness of observed wells. It provides periodic or seasonal results (Healy & Cook, 2002). The simplicity and low cost of the method make it popular worldwide for shallow groundwater studies (Addisie, 2022; Choi et al., 2007; Duah et al., 2021; Varni et al., 2013). For accurate use, the aquifer must be unconfined, with water moving freely vertically and laterally, and rainfall must be the only recharge source (Healy & Cook, 2002; Walker et al., 2019). This method can effectively show short-term groundwater responses to storms and is insensitive to water flow through unsaturated zones (Lutz et al., 2015). Different versions of the Water table fluctuation (WTF) method exist. This study uses a simplified approach for practical application. In this method, groundwater level rise indicates recharge, and level drop indicates recession. Recharge (R) is calculated by multiplying the change in water level (Δh) between two readings by the aquifer's Specific Yield (S_y) (5) (Healy & Cook, 2002):

$$R = S_y * \frac{\Delta h}{\Delta t} \quad (5)$$

Where h denotes the water level (m), S_y the Specific Yield and t represents the time (days).

2.7.1 Estimation of change in groundwater level (Δh)

Commonly, to accurately determine Δh, the antecedent recession curve is extrapolated to the point below the crest, where the groundwater level curve would have reached without precipitation (Delin et al., 2007). Besides this "graphical method" an alternative approach of calculating the water level rise from one day to the next, with a negative rise (a fall in groundwater level) as zero is known (Rutledge, 1998). This less subjective approach is used in this study, though it may underestimate recharge by not accounting for recession without recharge (Delin et al., 2007; Walker et al., 2019).

2.7.2 Specific Yield (S_y)

In groundwater recharge assessment and the WTF method, Specific Yield (S_y) is vital. S_y is the fraction of water drained by gravity from saturated rock or soil (Meinzer, 1923). It represents the water storage term and is time-independent. S_y is related to Specific Retention (S_r) and porosity (∅) and can be calculated with the following equation, where S_r defines the volume of water retained by the rock or soil (Healy & Cook, 2002) (6).:

$$S_y = \emptyset - S_r \tag{6}$$

S_y is crucial for estimating groundwater recharge from changes in groundwater levels (Healy, 2010; Healy & Cook, 2002; Sophocleous, 1991). Multiple methods should be used to compute S_y for accuracy (Abera Beyene et al., 2019). Besides the presented methods below, laboratory drainage experiments, type-curve or volume balance methods are other of many ways to obtain S_y. Most of them require more advanced experiments and are inapplicable with respect to the data gathered during this study (Lv et al., 2021). This study applies two main approaches and compares them with literature values. S_y parameters were estimated for topsoil (0 – 10 cm) and a lower horizon (30 – 40 cm) near groundwater observation wells.

2.7.3 Mechanical-analysis

One option to compute S_y in the top soil layer is by adapting (6) with equalizing S_r to the FC like mentioned in (Healy, 2010) leading to (7) with calculation of porosity shown in (8).

$$S_y = \emptyset - FC \tag{7}$$

$$\emptyset = \frac{PD-BD}{PD} \tag{8}$$

Where particle - (PD) and bulk (BD) density (in kg m^{-3}) are defining total porosity (∅) which stands in direct relation with the Field Capacity (FC) and S_y (Healy,

2010; Healy & Cook, 2002; Meinzer, 1923; Scanlon et al., 2002). Particle density solely was not estimated with collected data but taken from Abera Beyene et al., 2019.

2.7.4 Particle size-analysis

Another way to estimate S_y is suggested as by analysis of particle sizes (Abera Beyene et al., 2019). With knowledge of the soil texture, values for Specific Yield are derived from a trilinear graph after (Johnson, 1967) Figure (16). When overlapping a simplified soil classification triangle as in Figure (15) with the graph by (Johnson, 1967), the range of S_y for different soil types can be given in percent by the lines in Figure (16) (Richey et al., 2015).

Figure 15. USDA Soil texture triangle as in Richey et al., 2015

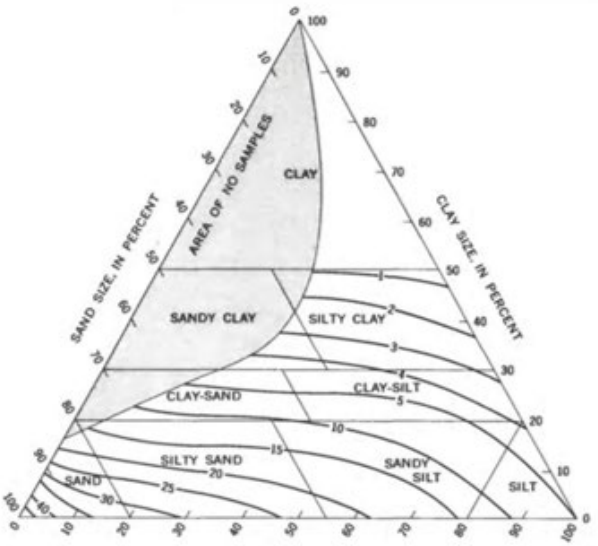

Figure 16. Sy according to USDA soil texture triangle as in Richey et al., 2015

3. RESULTS

3.1 Soil characteristics

Key findings of the soil characteristics data collected throughout the Mankran watershed, at various land use types and in 0 – 40 cm depth, are presented in the following section. Focus is set on parameters improving the understanding of groundwater recharge patterns. For a complete numeric compilation, refer to Appendix (2).

3.1.1 Texture

Statistical analysis of 55 samples at all plots, subplots and in 0 - 10; 10 - 20; 20 - 30 and 30 – 40 cm revealed overall high mean sand percentages reaching from about 60 – 80 %. The sampled textural classes in the watershed were Sand, Loamy sand, Sandy loam, Sandy clay loam and Sandy clay. Sandy clay loam and Sandy loam together covered almost 60 % of all measured spots. Loamy sand marked about 24 %, Sandy clay averaged 11 % and Sand was found in a fraction of about 7 % of all collected data Figure (17).

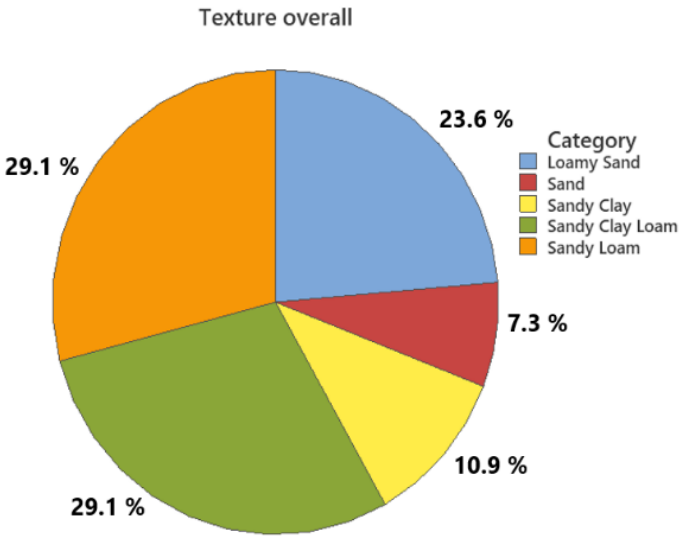

Figure 17. Dominant soil textures in Mankran watershed in percent

Samples from 0 - 10 and 30 – 40 cm depth were plotted in the USDA soil texture triangle Figure (18). There were, on average, higher clay percentages found at Barniekrom (midstream) and Kunsu (downstream) than at Mmrobem (upstream) and in 30 – 40 cm depth than at 0 – 10 cm.

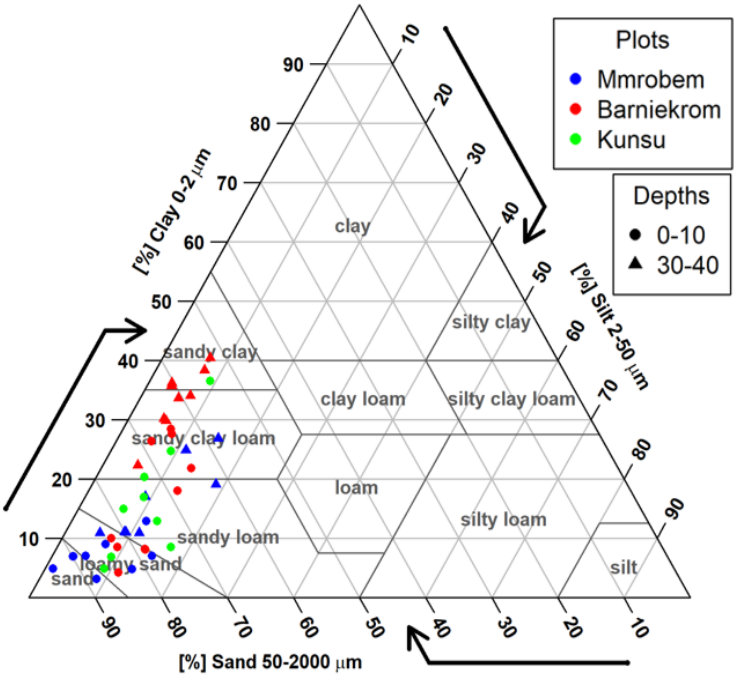

Figure 18. Soil samples categorized after USDA soil texture triangle

Scatterplots and field photos in Appendix (2) further display the findings of higher clay contents at 30 – 40 cm and varieties in landscape position. Overall, mean texture data values were subject to high standard deviations of up to 10 % Figures (19 – 20) Thus, a one way ANOVA of data collected at 0 - 10 and 30 - 40 cm respectively, tested significant differences in sand and clay fractions at plot and subplot level and depths. The null hypothesis (H0) of all means in fractions of sand being equal in the three different landscape positions (Kunsu, Barniekrom and Mmrobem) was rejected ($p = 0.00373$) for $\alpha = 0.01$. Similarly, $p = 0.000487$ showed significant differences in sand content according to depth. Thus, land use ($p = 0.0589$) was the only category suggesting fractions of sand being non - significant for $\alpha = 0.05$ or 0.01. Tuckey's HSD post hoc test then identified mean sand content in the upper parts (Mmrobem) as significantly higher than in the middle (Barniekrom) ($p = 0.002527$). Additionally, sand fractions were generally lower at 30 – 40 cm than at shallower depths ($p = 0.0004874$).

Those results are further underscored by the boxplots in Figure (19) revealing highest sand contents at Mmrobem and lowest in 30 – 40 cm depth at Barniekrom.

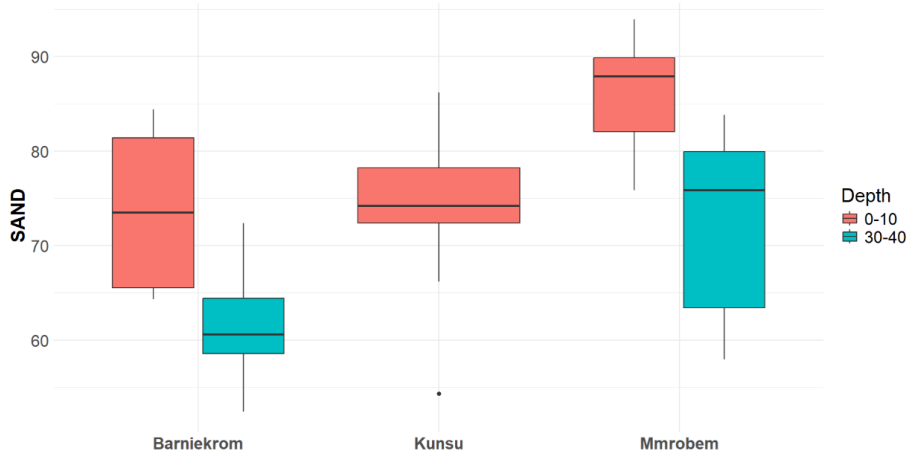

Figure 19. Boxplots of sand fractions in % varying with plots and different depths (cm)

The same statistical approach as well as Figure (20) revealed that clay contents varied within the watershed in a similar pattern as sand did. There were no

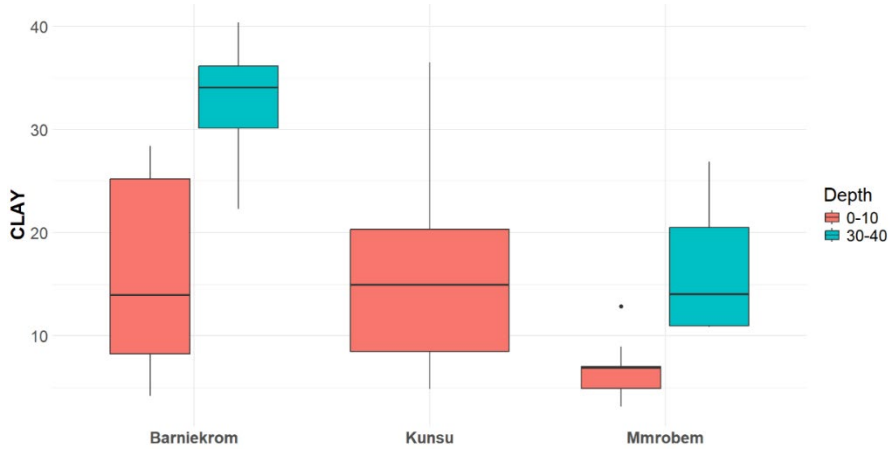

Figure 20. Boxplots of clay fractions in % varying with plots and different depths (cm)

significant differences between clay fractions in sampled land use types ($p = 0.161$) but in the areas from upstream to downstream ($p = 0.00117$) and according to the depth ($p = 0.00015$). The areal distinction was at Mmrobem (upstream) compared to Barniekrom (midstream) ($p = 0.0008250$), whereas clay contents at Kunsu (downstream) were not significantly different from the other plots. Opposite to sand, clay contents were higher in the middle of the watershed (Barniekrom) and in 30 – 40 cm while being lower at the upper area (Mmrobem) and in 0 - 10 cm from the surface.

3.1.2 Soil pH and organic matter

The same 45 samples analysed for soil texture at 0 - 10 and 30 – 40 cm were tested on pH and organic matter displaying a pattern throughout the watershed. As seen in Figure (21), at Barniekrom (midstream) and Mmrobem (upstream), the soil was acid and neutral, respectively indicating areal dependence. Samples at Kunsu (downstream), instead were reaching from acid to neutral presumably depending on land use type like the acid mining site.

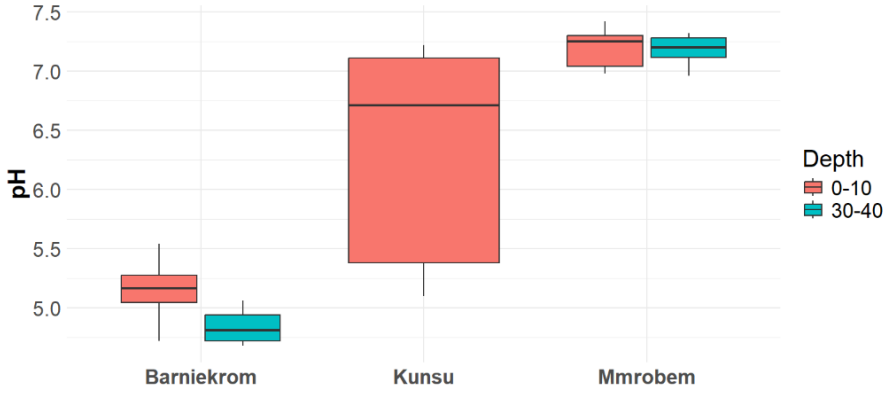

Figure 21. Boxplots of pH values at the plots and in different depths (cm)

Generally, soil pH did vary substantially within the land use types but one way ANOVA analysis explained in Figure (21) not depicted patterns. Not only at plot but also at subplot level, a p - value much smaller than $\alpha = 0.001$ (2e-16 and 3.51e-16) indicated statistically significant differences in pH. With $p = 0.0923$ instead, deviations solely due to varying depths were not proven to be as clear. Tuckey's HSD test further revealed significantly lower pH in the mining area than at any other subplot ($p = 0$ for both). Samples from built-up areas were characterized with higher pH values than plantain ($p = 0.005$) and cocoa ($p = 0.027$) sites. Latter did not differ significantly in pH ($p = 0.993$).

As depicted in Figure (22), organic matter contents varied with different land use types and depths. Built-up areas and the mining subplot revealed the lowest organic

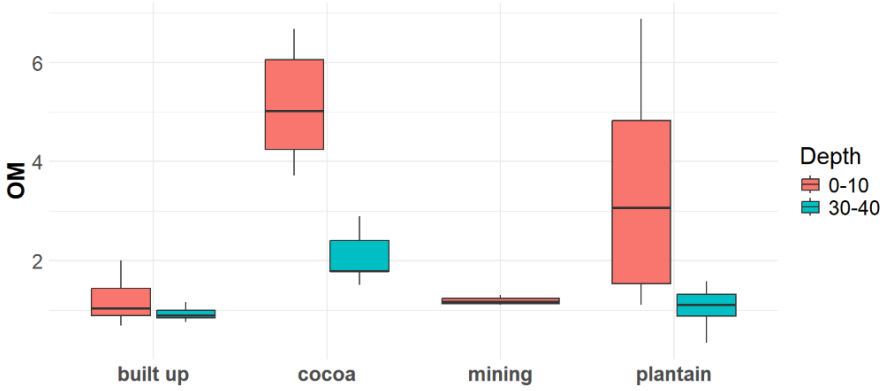

Figure 22. Boxplots of organic matter (OM) fractions in % at the subplots and in different depths (cm)

matter contents and the lower depths at the plantain fields (ca. 1 – 2 %). The highest percentages of organic matter content in both depths were found at the cocoa subplots (ca. 4 – 7 %). More scattered samples at the plantain subplots in 0 – 10 cm depth also reached high fractions of about 7 %. Overall, organic matter content was higher at plantain and cocoa sites than at the built-up and mining subplots, where 2 % was not exceeded. The results displayed for the mining site were based on three samples in 0 – 10 cm depth. Organic matter content decreased with increasing depth throughout all subplots except from the mining site, where no data from 30 - 40 cm was collected. However, data in lower layers was generally more homogenous than in shallower depths.

3.1.3 Bulk density

47 samples in 0 - 10 and 30 – 40 cm depth revealed correlations of bulk density with land use type and depth. As shown in Figure (23), bulk densities (g cm^{-3}) were, on average, higher at 30 – 40 cm than at 0 – 10 cm. The highest values in shallow depths were found at built-up (ca. 1.6 – 1.7 g cm^{-3}) and plantain (reaching 1.8 g cm^{-3}) and lowest at cocoa subplots (ca. 1 – 1.5 g cm^{-3}). Bulk density in 30 – 40 cm was similar throughout all land use types, reaching approximately 1.4 – 1.8 g cm^{-3}. With

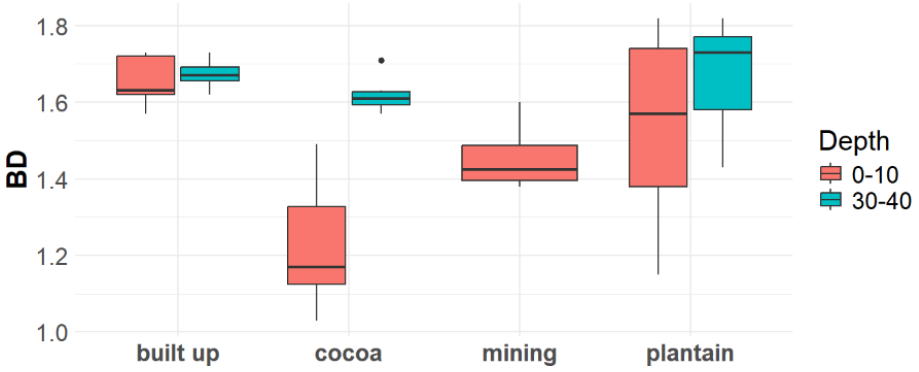

Figure 23. Boxplots of bulk density (BD) in g cm-3 at the subplots and in different depths (cm)

ca. 1.2 – 1.8 g cm^{-3} in 0-10cm and 1.4 – 1.8 g cm^{-3} in 30 – 40 cm, plantain subplots showed higher variations than others did in the same depths. Data collected in built-up areas is consistent in both depths. The only outlier was 1.71 g cm^{-3} at the 30 – 40 cm cocoa subplots. At the mining area, data in 30 – 40 cm was missing. One – sided ANOVA analysis with $\alpha = 0.05$ showed no significant effect of plots on bulk density ($p = 0.28$). It did however support the in Figure (23) depicted effect of land use type ($p = 0.0033$) and depth ($p = 0.0026$) with $\alpha = 0.01$ as threshold.

3.1.4 Field-saturated hydraulic conductivity (Kfs)

Generally, built-up areas had the lowest infiltration rates reaching from around 10 to 40 mm h^{-1}, with one outlier in the upstream-agroforest area (Mmrobem) stabilizing at ca. 60 mm h^{-1} after more than two hours Figure (24). More homogenous values than other land use types were measured in plantain fields throughout the whole watershed. They were found to have slightly higher magnitudes as the built-up subplots ranging from 10 to 60 mm h^{-1} Figure (25). At the cocoa subplots, two outliers at around 40 mm h^{-1} in the area of Barniekrom

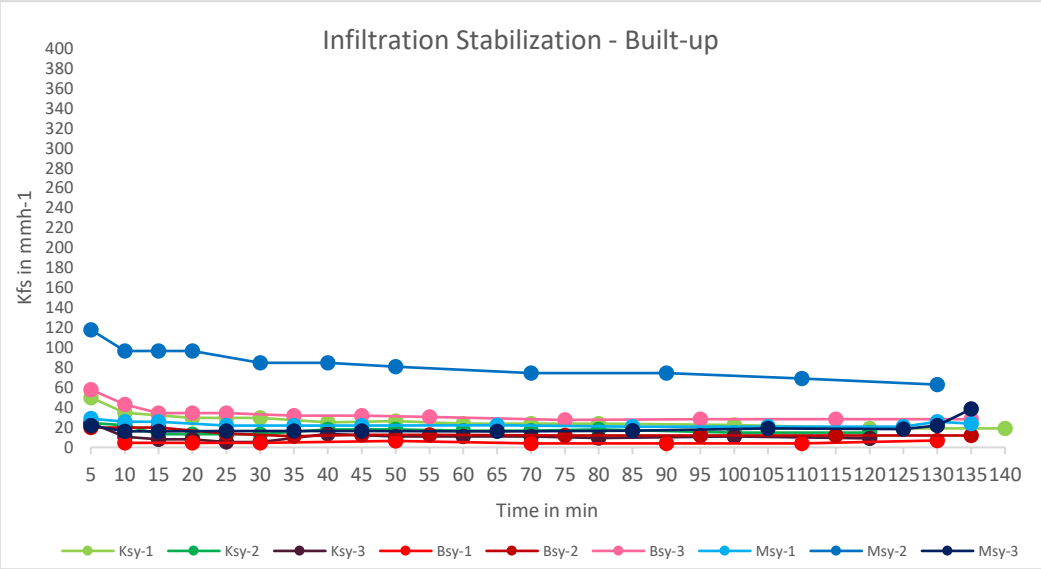

Figure 24. Infiltration measurements at the built up subplots in Kunsu (Ksy), Barniekrom (Bsy) and Mmrobem (Msy)

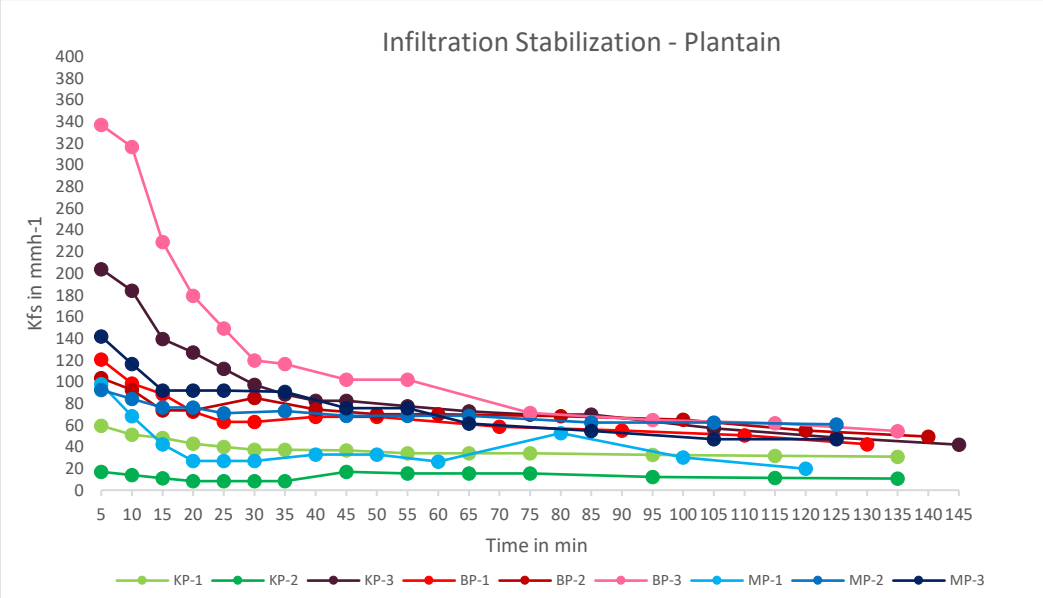

Figure 25. Infiltration measurements at the plantain subplots in Kunsu (KP), Barniekrom (BP) and Mmrobem (MP)

(midstream - agriculture) and 300 mm h^{-1} at Mmrobem segregated from the other four infiltration measurements, ranging from 110 to 160 mm h^{-1} Figure (26).

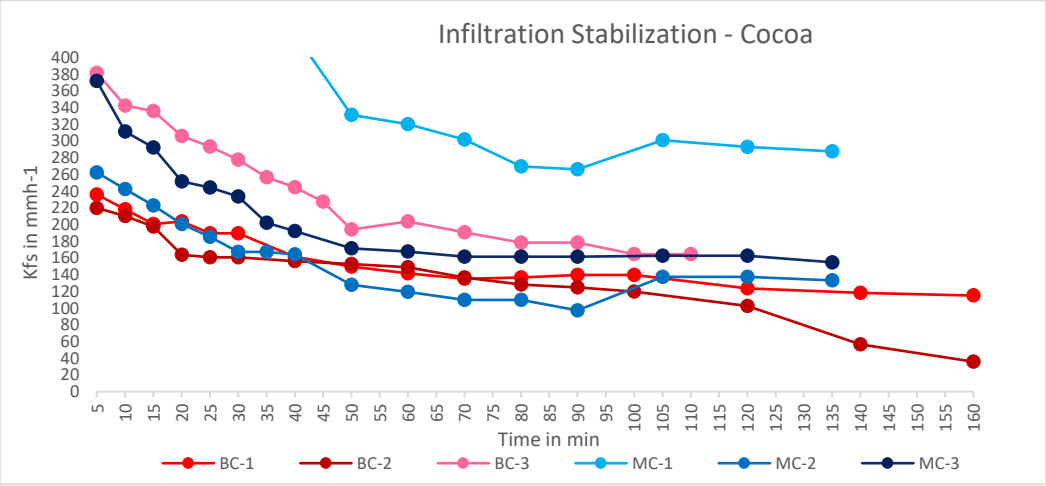

Figure 26. Infiltration measurements at the cocoa subplots in Barniekrom (BC) and Mmrobem (MC)

Averaged, stabilized Kfs rates revealed the fastest infiltrations at cocoa sub plots, as shown in Figure (27). Measurements in the cocoa fields delivered around 120 - 200 mm h^{-1}, or more than four times the rates at plantain subplots (20 - 50 mm h^{-1}) and up to 10 times compared to 15 – 40 mm h^{-1} at built-up areas. The agroforest

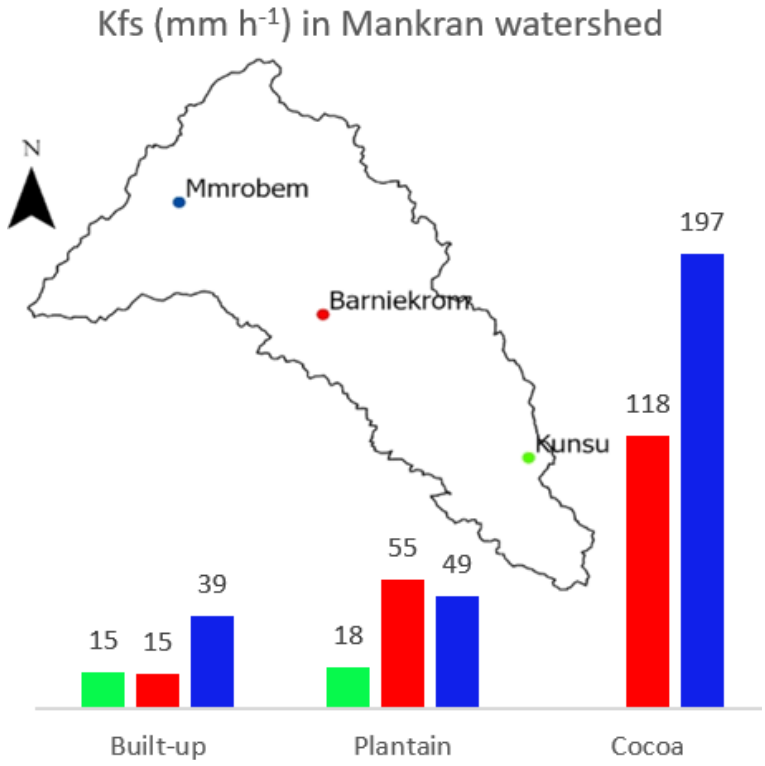

Figure 27. Averaged Kfs values throughout plots (downstream/Kunsu = green; midstream/Barniekrom = red; upstream/Mmrobem = blue) and subplots (Built-up, Plantain, Cocoa)

area plot (Mmrobem) in the upper catchment revealed the highest infiltration numbers besides a lower average in the plantain field, ranging from around 40 – 200 mm h^{-1}. Calculated Kfs values in the downstream area (Kunsu) were the lowest with 15 – almost 20 mm h^{-1}. Overall, a decreasing trend from the upper to the lower plots of the catchment and from cocoa to built-up subplots prevailed. Thus, Kfs rates in the Mankran watershed vary with landscape position and land use type.
In summary, high organic matter fractions combined with low bulk densities in 0 – 10 cm were in accordance with higher infiltration rates at plantain and cocoa subplots. Soil pH values in neutral range were primarily found in the area with highest infiltration rates, namely upstream at Mmrobem. Samples in this area were also statistically significant higher in sand and lower in clay content than the others. Slightly acid soils mid – and downstream along with more compacted topsoil in built up areas came along with lower infiltration rates.

3.2 Estimation of groundwater recharge

3.2.1 Rainfall data

Rainfall data obtained by citizen scientists was the basis for application of both methods used for groundwater recharge estimation. Following Figure (28) is displaying monitored rainfall patterns (mm) in all three communities from June 2023 – July 2024.

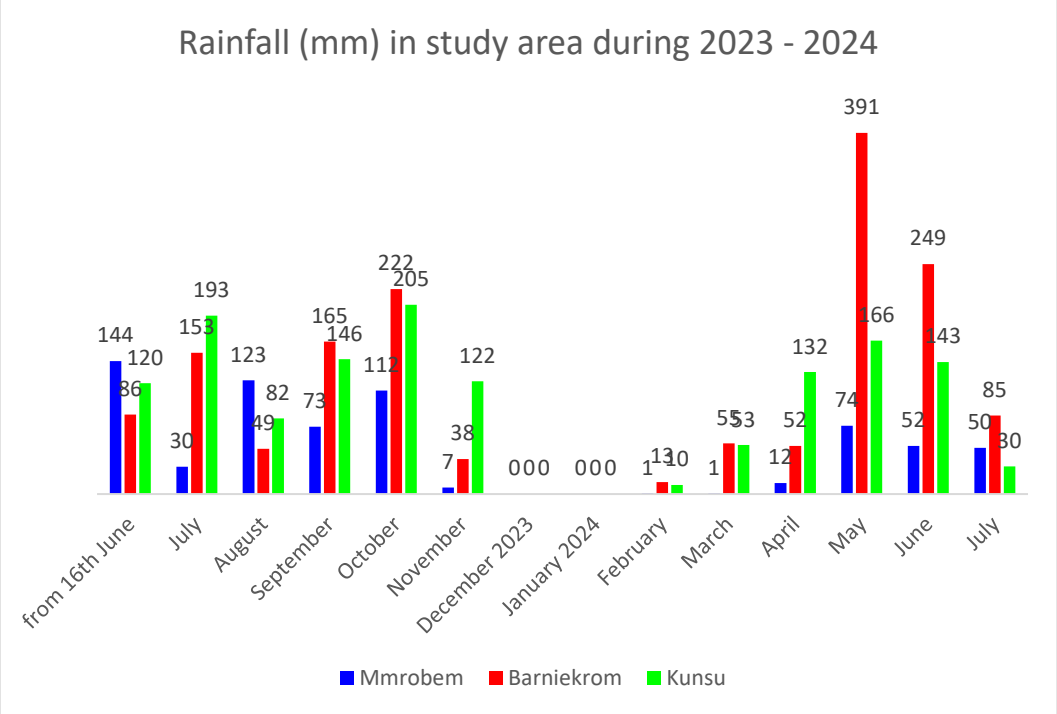

Figure 28. Rainfall in all three communities from June 2023 - July 2024

Accumulated seasonal rainfall averaged for the entire watershed was 700 mm from mid of June 2023 – end of November 2023 and 500 mm for March 2024 – July 2024. Thus, a total of about 1200 mm rainfall was collected during the documented raining periods from 2023 – 2024. During 2023, amounts at the downstream area (Kunsu) are with about 900 mm much higher than midstream (Barniekrom) with 700 mm and upstream (Mmrobem) with 500 mm. Besides no rain during the dry period from December 2023 – January 2024, rainfall was overall lowest at the end of the minor raining season in November and towards the beginning of the major raining season in March/April. The highest record was about 400 mm at Barniekrom in May 2024. Overall, rainfall patterns at the three communities differ less during 2023 than during 2024. With the exception of June and August in 2023, collected rainfall amounts at Mmrobem were lower than at the others.

1.1.1 Groundwater recharge from chloride mass balance

Observation data gathered within the TAFS – WCA project by IWMI, delivered chloride concentrations in rain-, surface- and groundwater at Barniekrom (midstream) and Mmrobem (upstream) Figures (29, 30, 32). Chloride concentrations at Kunsu (downstream) were not included for estimation of groundwater recharge since there was no stream gauge measuring flowrate for surface runoff at the lower part of that area Figure (9) (Adusei-Gyamfi et al., 2023). No rain in December and January and contaminated samples in July 2023 at both communities and March 2024 at Mmrobem solely, resulted in missing data in Figures (29, 30, 32). Overall, chloride in rainwater was following similar trends at both communities throughout the entire measuring period. Chloride in rainwater at both communities was up to twice as concentrated in June and August 2023 (20 – 40 mg L^{-1}) as during February – July 2024 (5 – 15 mg L^{-1}) as it was decreasing towards the end of the minor raining season in 2023. From February 2024 on, concentrations slightly increased again with no major fluctuations until 10 mg L^{-1}

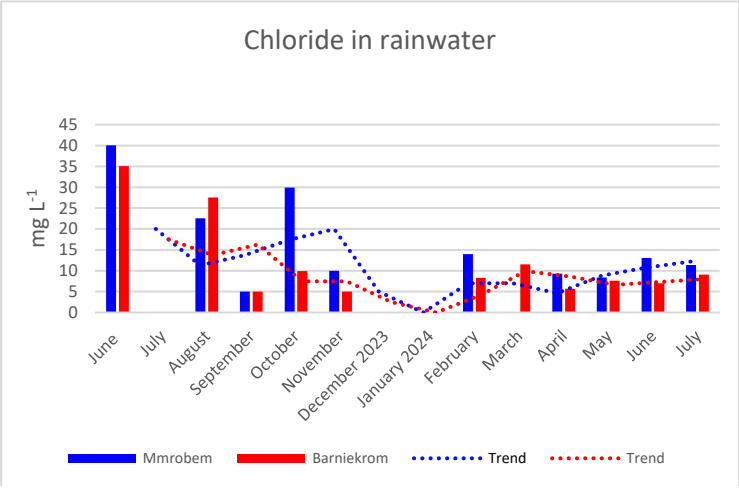

Figure 29. Chloride concentrations (mg L^{-1}) in rainwater

at Mmrobem and slightly less at Barniekrom at the end of the major raining season in 2024. With the exception of August 2023, chloride was overall more concentrated in rainwater collected at Mmrobem.

As seen in Figure (30), chloride concentrations in the groundwater wells were rising from ca. 20 mg L^{-1} (Barniekrom) and 50 mg L^{-1} (Mmrobem) in June 2023 to ca. 100 mg L^{-1} (Barniekrom) and 240 mg L^{-1} (Mmrobem) in October 2023. From the

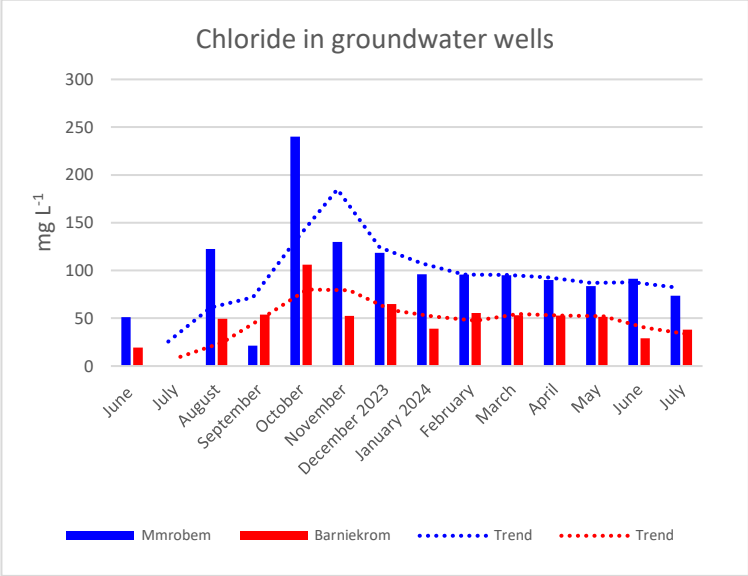

Figure 30. Chloride concentrations (mg L^{-1}) in groundwater wells

end of the minor raining season in November 2023 onwards, chloride concentrations were decreasing slightly, stabilising at 80 – 90 mg L^{-1} for Mmrobem and at about 50 mg L^{-1} for Barniekrom. Only towards the end of the major raining season of 2024, especially at Barniekrom but also at Mmrobem, concentrations decreased to ca. 70 mg L^{-1} and 40 mg L^{-1} at Mmrobem and Barniekrom respectively.

Thus, chloride concentrations in groundwater are potentially indirect proportional to the average fluctuating water table from groundwater wells in those communities shown in Figure (31).

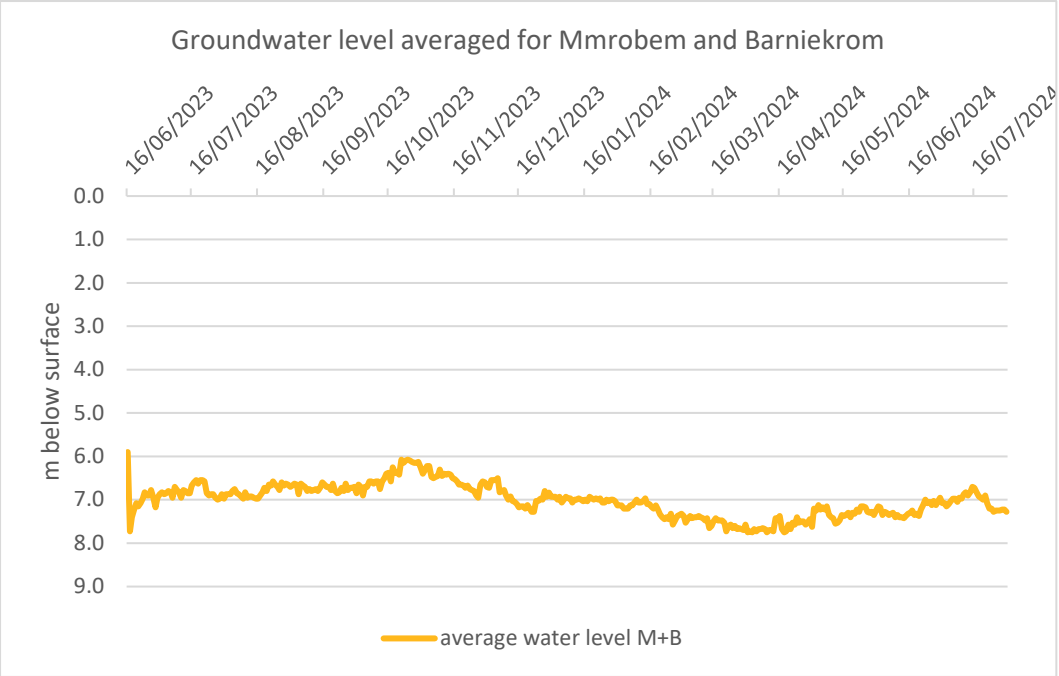

Figure 31. Average groundwater levels in observation wells BGW 1-3 and MGW 2

However, dominant chloride concentrations in Mmrobem, as detected in rain- and groundwater, repeated in surface water measurements Figure (32) While values at Mmrobem, like in the groundwater well, were peaking over 100 mg L^{-1} in November/December 2023, chloride concentrations at Barniekrom remained quite stable at about 30 mg L^{-1} throughout October 2023 – June 2024. For Mmrobem, a

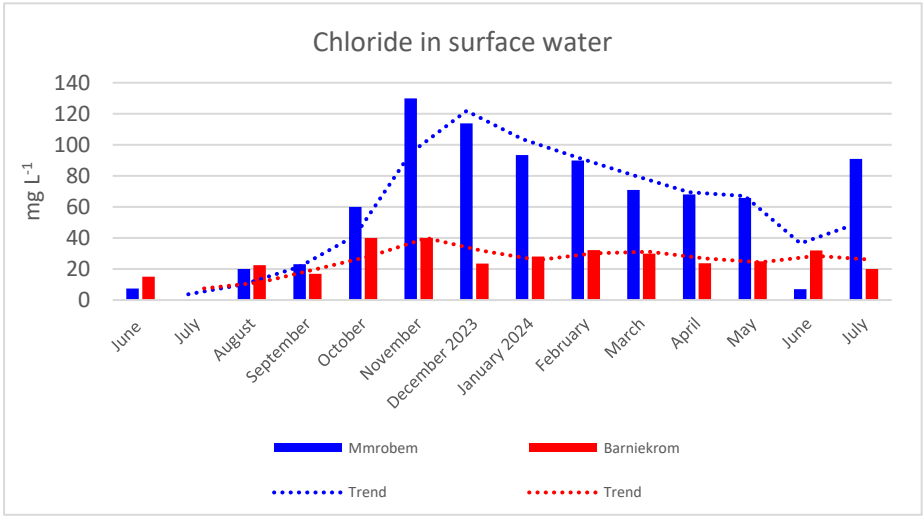

Figure 32. Chloride concentrations (mg L^{-1}) in surface water

gradual decrease ended with a global low of 7 mg L^{-1} in June 2024 followed by a sudden increase to 90 mg L^{-1} in July 2024.

The following Figure (33) depicts the monthly surface flowrates at the gauges in Kunsu (KSW) and Barniekrom (BSW) transporting chloride away. As seen in the map, the red area is part of the green area flowing through KSW. With the exception of June - August 2023, flowrates at BSW were almost constantly, significant lower than at KSW. A clear pattern shows increasing flowrates towards the end of the minor raining season at both gauges, peaking at over 70 mm (KSW) and about 20 mm (BSW) following heavy rainfalls (75 - 200 mm) from June – October 2023. After the dry period, there was an increment of up to 6 mm (KSW) and 4 mm (BSW) in June 2024 responding to the major raining season starting from March and almost 200 mm precipitation during May 2024.

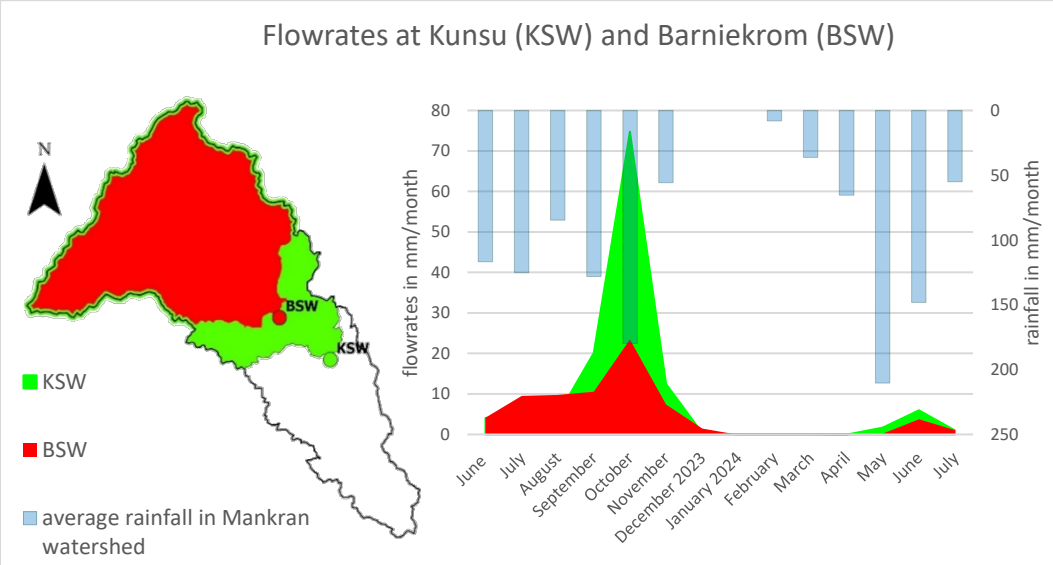

Figure 33. Flowrates at the stream gauges in Barniekrom (BSW) and Kunsu (KSW) responding to rainfall

As shown in Table (3), the seasonal recharge from June until November 2023, computed by the CMB, strongly depends on the chosen runoff regime. It ranges from ca. 10 % at Mmrobem to 19 % at Barniekrom, considering surface flow rates at Kunsu (KSW) and reaches ca. 15 % at Mmrobem to 25 % at Barniekrom using surface flow rates from Barniekrom (BSW) respectively. Aerial averaged recharge rates range 10 - 17 % of the seasonal precipitation. Instead for the major raining season in 2024, recharge was much lower between 2 – 3 % with runoff from KSW and 6 – 9 % with runoff from BSW. No matter the runoff regime, recharge at Barniekrom was consistently higher than at Mmrobem. The margin reached from 9 – 10 % during 2023 and down to just 1 – 3 % in 2024. A total of 12 – 22 % (KSW) or 21 – 34 % (BSW) during the documented raining periods of 2023 – 2024 recharged into the groundwater body.

Table 3. Groundwater recharge estimations by CMB

16th June – 31st November 2023		**Recharge according to different runoff regimes**		**1st March – 31st July 2024**		**Recharge according to different runoff regimes**	
Location	**Rainfall in mm**	**Runoff from KSW**	**Runoff from BSW**	**Location**	**Rainfall in mm**	**Runoff from KSW**	**Runoff from BSW**
Mmrobem	868	10 % (72 mm)	15 % (106 mm)	**Mmrobem**	189	2 % (8 mm)	6 % (32 mm)
Barniekrom	713	19 % (131 mm)	25 % (172 mm)	**Barniekrom**	832	3 % (17 mm)	9 % (47 mm)

3.2.2 Groundwater recharge from water table fluctuations

The essential parameter for application of the WTF method was Specific Yield. The following Table (4) depicts averaged S_y values obtained through application of Mechanical – and Particle-size analysis as in Figure (16) along with comparable data from literature (Loheide II et al., 2005; Obuobie et al., 2012; Richey et al., 2015). Averaged Field Capacities as basis for the Mechanical-analysis are shown as well. The complete results from pressure plate analysis including Wilting Point (WP) are attached in Appendix (2).

Table 4. Variations of Specific Yield (Sy) and Field Capacity (FC)

		FC in %			**S_y values in %**			
Plot in Mankran watershed	**Geology**	**0-10 cm**	**30-40 cm**	**Prevalent texture**	**Mechanical Analysis** (particle density from Abera Beyene et al., 2019)	**Particle Size Analysis** (Richey et al., 2015)	**Reverse educing method** (Loheide II et al., 2005)	**Geology** (Obuobie et al., 2012) after Sinha and Sharma, 1988
Kunsu	Birimian Supergroup	19.0	20.6 (20-30 cm)	Sandy Loam	15.6	22.5	17	3.0
Barniekrom	Eburnean Plutonic Suite	10.6	14.4	Sandy Clay Loam	22.1	8.5	7.2	3.5
Mmrobem	Tarkwaian Group	17.6	15.8	Sandy Loam/Loamy Sand	16.0/no data	22.5/no data	17/26	3.0

All the depicted data in Table (4) was in line with prevailing texture and geology in the Mankran watershed. It reveals great variability of FC and S_y. In the lower section (Kunsu) FC was almost 20% throughout 0 – 30 cm depth. Values in the upper, sandier, section (Mmrobem) were close to 18 % in the topsoil and 16 % in the deeper layer. Midstream (Barniekrom) with higher clay fractions, revealed 10.6 % in shallower and 14.4 % in deeper layers. Overall, Mechanical - and Particle Size Analysis delivered the highest S_y values along with literature values from (Loheide II et al., 2005). The biggest gap within this group was midstream at Barniekrom. S_y ranged from 7.2 over 8.5 to 22 %. Literature values from suitable geologic material were generally much lower down by almost 20 %. Such categorization after weathered material like green schists (Birimian and Tarkwaian Groups) and granite (Eburnean Plutonic Suite) led to values of 3 - 3.5 %. Further important for application of the WTF method are the monitored ground water levels in the 6 observation wells as in Figure (34).

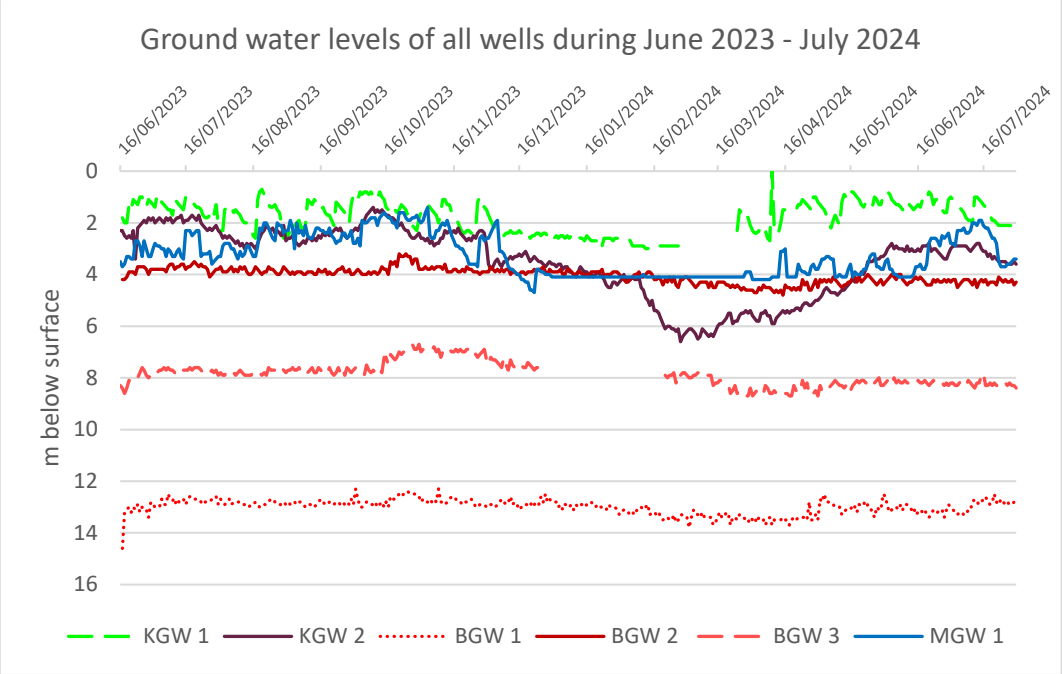

Figure 34. Water levels of all observation wells in Mankran watershed

During the whole period, depths at wells in Kunsu and Mmrobem as well as BGW 2 in Barniekrom were mostly within 4 m. From beginning of the dry season in December 2023 until the end of February 2024, they were lowering down as far as 6 m at KGW 2. Then, especially KGW 2 and MGW 1 followed the beginning of the major raining season with increasing water levels until peaking around June and July 2024. From mid of July onwards, water tables were lowering down again. Two wells in the midstream section (Barniekrom) were reaching deeper levels of around 8 m (BGW 3) and 13 m (BGW 1). Starting from mid of October until the end of 2023, the water table in BGW 3 was rising over 7 m to the ground. Within the dry

season, namely from December 28th to February 20th, part of BGW 3 collapsed causing temporary monitoring stop as during February/March 2023 at KGW 1. After that time, BGW 3 reached groundwater levels in similar order as before October 2023. BGW 1 was not subject to outstanding fluctuations. However, less significant than at the shallower wells, water levels at BGW 1 gradually lowered down during the dry season as well. From around May 2024 on, CS documented a gradual rise in water table with minor fluctuations to similar levels as before the dry season. The relation between groundwater levels and seasonal dependent rainfall is shown in the following Figure (35). Overall, there was a recurring correlation between averaged well levels and averaged precipitation. That to say, water levels were rising after precipitation events and falling during times of drought. This pattern was most clearly visible after consecutive rainfall events during the end of June and beginning of October 2023 followed by dry periods in August and November 2023. It was even more evident in 2024, when water tables gradually rose with the beginning of the raining season.

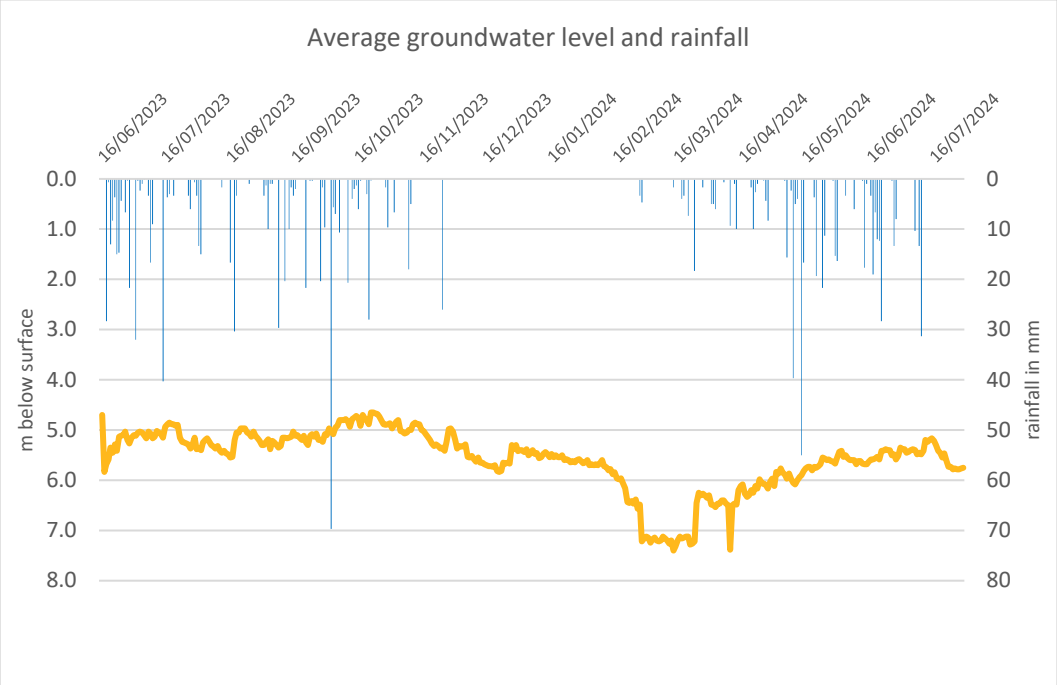

Figure 35. Average water level of all observation wells related to average precipitation in Mankran watershed

The fluctuations of water levels in 6 monitored wells figure (all gw wells), along with presented values for S_y Table (4) and collected rainfall data Figure (29) allowed estimation of seasonal groundwater recharge using WTF method. The recharge rates were strongly depending on S_y values with some results even exceeding collected rainfall amounts. A complete compilation of all recharge values is in Appendix (3).

The Table (5) on page 50 depicts recharge rates below 100 % of the monitored rainfall from mid of June 2023 – November 2023 and March 2024 – July 2024 respectively. Using S_y from Sinah and Sharma, 1988, results were ranging from 8 % (midstream) to about 20 % (up-/downstream) with an average of 16 % for the entire watershed. Higher S_y values delivered data below 100% for the midstream section solely, ranging from 14 – 44 % with an average of 25 %. For the major raining season in 2024, geologically determined S_y estimated 9 % for midstream, 23 % for upstream and 35 % in the downstream area. Higher S_y estimations again delivered results below 100 % for Barniekrom solely. Taking S_y from Loheide II et al., 2015 resulted in 14 %, trilinear graph by Johnson, 1967 in 18 % and mechanical analysis delivered 44 %. Overall, estimated recharge with geologically determined S_y resulted in significantly lower rates than for the others. Groundwater recharge in the midstream area (Barniekrom) was substantially lower than down- and upstream (Kunsu and Mmrobem) in both periods.

Table 5. Groundwater recharge estimations by WTF

Location	16th of June – 31st of November 2023					1st of March – 31st of July 2024				
		Recharge according to different Sy values					Recharge according to different Sy values			
	Rainfall in mm	Mechanical Analysis	Particle Size Analysis	Reverse Educing Method	Geology	Rainfall in mm	Mechanical Analysis	Particle Size Analysis	Reverse Educing Method	Geology
Kunsu	868				21 % (144 mm)	524				35 % (180 mm)
Barniekrom	713	44 % (300 mm)	18 % (123 mm)	14 % (96 mm)	8 % (55 mm)	832	47 % (242 mm)	19 % (99 mm)	15 % (77 mm)	9 % (44 mm)
Mmrobem	489				20 % (135 mm)	189				23 % (117 mm)
Average all	690				16 % (111 mm)	515				22 % (114 mm)

With Sinha and Sharma, 1988, the total recharge from 2023 – 2024 was estimated at 17 – 44 % for the midstream area and 43 % in the upstream section. Those numbers opposed 12 % for the up- and 22 % for midstream section calculated by CMB. WTF was estimating recharge at Kunsu as well. The sum from 2023 – 2024 resulted in 56 % with 21 % in 2023 and 35 % in 2024 respectively. Seasonally, projections by WTF clearly exceeded those by CMB. During June – November 2023, CMB projected 10 % at Mmrobem and 19 % at Barniekrom while WTF led to 20 % at Mmrobem and 8 – 44 % at Barniekrom. March – July 2024 revealed a similar pattern. CMB dated groundwater recharge at 2 % for Mmrobem and 3 % for Barniekrom while WTF had 23 % for Mmrobem and 9 – 47 % for Barniekrom. Figure (36) visualizes the groundwater recharge according to different runoff regimes and S_y with: KSW (CMB results with runoff from KSW); BSW (-"- with runoff from BSW); WTF with (M = mechanical S_y; P = S_y via particle size-analysis; R = S_y via reverse educing method; G = S_y through geology). Lighter colour = June – November 2023; darker colour = March – July 2024

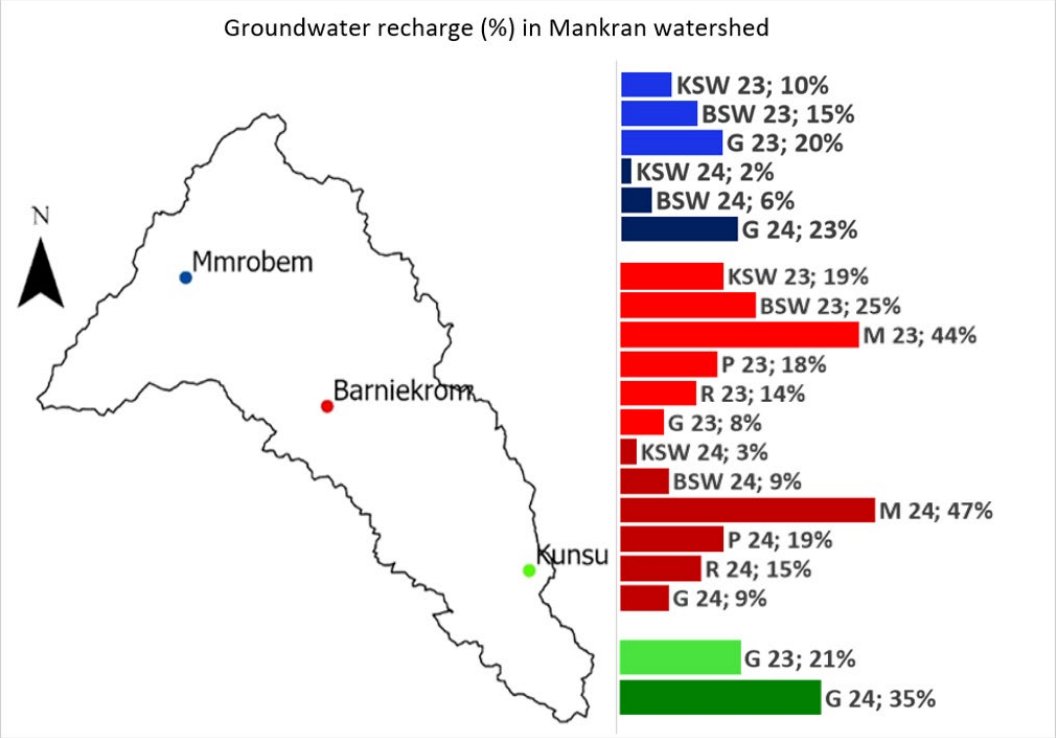

Figure 36. Compilation of groundwater recharge estimations by CMB and WTF according to landscape position in Mankran watershed

4. DISCUSSION

4.1 Results in context to literature

Initial expectations for this research were to improve knowledge of shallow groundwater flow patterns in the Mankran micro watershed. Collected soil physical properties influencing groundwater recharge revealed inhomogeneity throughout the watershed with variations according to plots, subplots and depths. High sand fractions over 60 % suggested porous soils with consequently increased permeability and lower water holding capacity. The upstream community (Mmrobem) distinguished from mid- (Barniekrom) and downstream (Kunsu) with statistically significant higher sand contents. Clay fractions, with opposing characteristics to sand, were greater at the middle and lower sections of the watershed as well as in higher depth. Texture in the watershed classified as Sandy loam, Sandy clay loam and Loamy sand with 30 % each. Those findings were supplemented by comparable textures in the cocoa agroforest area around Nkrankwanta and Diabaa as shown in Fosu-Mensah et al., 2016 Table (1).

Statistical analysis detected dependency of soil pH on area and land use type. Commonly known as indicator for soil aggregation, chemical, microbial and root activity, soil pH around neutral (6 - 7) is ought to have better soil structure with larger pore spaces, allowing for more efficient infiltration and percolation of water. The agriculturally dominated midstream area (Barniekrom) turned out as the most acid (pH around 5) favouring dispersion and compaction of soil. The same goes for the mining subplot at Kunsu (downstream) with the on average lowest pH (around 5) of all land use types. In accordance with the wide range of pH found at all the subplots, acid conditions (pH around 5) were also found in plantain fields at a research site in Biemso, in proximity to Kunsu Table (1). Sampling at an abandoned mining site in Afiesa however did reveal a higher pH of 6. Upstream (Mmrobem) and at the built up areas on the other side, dominated the highest pH (around 7) promising conditions favouring groundwater recharge. As cited in Table (1), studies in western Ghana found soil pH in cocoa fields at 7 – 8. Cocoa and plantain subplots in the Mankran watershed reached neutral pH as well but were more volatile going down until around 5.

Strongly tied to soil pH and microbial decomposition, organic matter content further improves soil structure, permeability and infiltration rates while reducing surface runoff (National Research Council, 1994). Such is expected at the cocoa and plantain fields where organic matter from 4 – 7 % and up to 7 % were the highest. No matter the land use type, organic matter content decreased significantly with depth. This pattern suggests that organic matter inputs from surface vegetation are more significant than subsurface inputs. Overall, the sampled values are in line with most comparable data presented in the background section ranging between 0.5 – 4 %. However, higher fractions of 7 % in cocoa fields are still comparatively low to about 10 % at a cocoa field in Diabaa or 12 - 13 % at woodland and forest predicted by Bargués-Tobella et al., 2024 via MIR Spectroscopy Table (1).

A general indicative of compaction is bulk density. Human presence is affecting root penetration and hindering water movement as seen in greater densities within the soil profile in the built up areas. The generally expected increment in compactness with depth was not as evident at all land use types. There were no or just minor differences at built up and plantain areas but a clear decrease towards shallower depth at the cocoa subplots. Disregarding locational differences in texture, namely clay and sand fractions, bulk density measurements showed lowest compactness at cocoa (1 – 1.5 g cm $^{-3}$) subplots. A low topsoil bulk density in cocoa fields is also shown in table (background) with only 1.10 g cm $^{-3}$ in 0 - 20 cm. Data from various land use types with similar soil textures as in the Mankran watershed range around 1.50 g cm $^{-3}$ in 0 - 20 cm Table (1). Those set the retrieved samples reaching from 1.2 – 1.8 g cm $^{-3}$ in logical perspective.

The all-encompassing factor showing the potential for groundwater recharge is the topsoil infiltration rate. Conducted measurements delivering field-saturated hydraulic conductivity (Kfs) were seemingly responding to the compaction, pH and organic matter content of the soil. More porous, sandy soils with near neutral pH found in the upstream area (Mmrobem) delivered the highest infiltration rates of ca. 40 mm h^{-1} in built-up and about 200 mm h^{-1} in cocoa subplots as well as the 2nd highest with ca. 50 mm h^{-1} at the plantain field. Additionally, water at the cocoa fields was infiltrating 4 to 10 times as fast as at the other land use types. It is therefore suggested that especially porosity and organic matter contents, promoted through neutral pH values, substantially influence Kfs. The globally insufficient understanding of hydrological processes in cocoa agroforests as mentioned in Farrick & Gittens, 2023, did not allow comparison of cocoa infiltration results with related literature. The variety of methods and terms to estimate and designate infiltration rates (K, Kfs, etc.) further distort possible contrast. However, Bargués – Tobella et al., 2024 estimated ca. 60 mm h^{-1} in a non-specified forest on Sandy loam and ca. 10 mm h^{-1} in woodland on Sandy clay loam using the same method as

this study did. A metastudy from Gupta et al., 2021, averaged 6 and 30 mm h^{-1} for Sandy clay loam and Sandy loam while 55 mm h^{-1} for Loamy sand. Further data shown in Table (1), dates infiltration on Silt loam with max. 24 mm h^{-1} in plantain fields and at 30 – 60 mm h^{-1} in fallow land. Overall, comparison reveals much lower infiltration rates at similar texture types than found in the cocoa fields in the Mankran watershed. However, values in built up areas (15 – 40 mm h^{-1}) and plantain fields (18 – 55 mm h^{-1}) fell in the same range as data from literature.

The two applied methods delivered different groundwater recharge results. A hereby confirmed observation by Walker et al., 2019 states that recharge computed by the CMB is ought to be delivering rather conservative numbers meaning a lower recharge than the WTF. Over the whole period from June 2023 – July 2024, CMB averaged 12 % for the up- and 22 % for the midstream area, under runoff regime from KSW. Missing runoff data in the downstream area (Kunsu), did not allow recharge estimation by CMB. The WTF method instead, estimated recharge for Kunsu at 56 % and therefore the overall highest areal recharge in the Mankran watershed. Further, it delivered 17 - 43 % for the mid- and 44 % for the upstream section. With the WTF estimating recharge more than three times as high as CMB, the variation of results in the upstream area (Mmrobem) was significant. Only the midstream section (Barniekrom) revealed similar tendencies, with 17 – 44 % by WTF and 22 % by CMB. Consequently, averaging uniform recharge for the entire area was not possible. On a seasonal level, recharge rates by WTF were again much higher in both areas (two – more than 10 times) than those by CMB. In summary, the methods did rarely deliver the same results. Not least since the majority of the estimations by WTF projected more than 100 % recharge. As foreseen, the CMB delivered rather conservative rates compared to the WTF. Recharge estimations in Ghana, presented in the background section, revealed up to ca. 30 % recharge through rainfall with a benchmark set at roughly 10 %. Variations within WTF, CMB and others were ranging between 0 and 30 %. Presented results in this work were therefore in accordance with those findings. Overall, results from the CMB were more often within this benchmark than results from the WTF.

4.2 Limits of methods and material

The actual groundwater recharge estimation by the WTF method was strongly tied to the Specific Yield (S_y). Comparison with values from other studies as in table (results), revealed substantial variations in S_y according to the method of estimation. The results from performed mechanical – and particle size analysis together with literature using reverse educing method strongly deviated up to 20 % from geological estimations of around 3 %. Johnson, 1967 did not develop the trilinear graph for estimation of S_y in tropical conditions, the applicability of the

particle size-analysis in the Mankran watershed is therefore questionable. Different classification practices such as by FAO and USDA additionally affect comparability to other textural data. While this study used the USDA soil texture triangle, related work might have used other classification methods distinguished by number and boundaries of textural classes. After all, solely using texture to define S_y delivered incongruent results.

The mechanical analysis demands knowledge of the Specific Retention (S_r) for estimation of S_y. For practical reasons, S_r was interchanged with soil Field Capacity (FC) as suggested by Healy, 2010. Pressure plate analysis applying standard pressures of 0.33 bar for FC and 15 bar for WP respectively, as conducted for this study, commonly delivers FC and Wilting Point (WP). While state of the art methods use undisturbed soil samples for pressure plate analysis, the lab used for this study took disturbed, loose samples. This adapted method represents a major unreliability for the results of the pressure plate analysis. Since designated pressure plate samples were solely tested on FC and WP and not on their texture, testing the reliability of using disturbed soil samples was difficult. However, an exception was found at the downstream area (Kunsu), where all other soil samples classified as Sandy loam. Therefore, a FC of ca. 19 - 20.6 % in that area is similar to Gupta et al., 2021 averaging 24.2 % for the same texture. FC for the midstream (Barniekrom) with predominantly Sandy clay loam was 10.6 % compared to 28.7 % from Gupta et al., 2021. Upstream (Mmrobem), where Loamy sand and Sandy loam were equally dominant, 13.1 – 18.4 % are opposing 17.3 – 24.2 % from Gupta et al., 2021. The continuous gap between sampled FC and data from literature suggests an inaccuracy through uncommon pressure plate analysis.

Rainfall data collected by citizen scientists varied substantially between Mmrobem and the lower two communities. The watershed average of about 1200 mm from 16th June 2023 – 31st July 2024 lies at the lower end of the climatic spectrum presented in the methods section. Kunsu recorded the highest precipitation in 2023 followed closely by Barniekrom. In 2024, there were remarkable differences between the three sites. A margin of more than 300 mm separated collected rainfall amounts at Barniekrom from Mmrobem. Although climatic conditions favour sudden cloudbursts, the gap seems very big. Not least since the distance between those two communities marks roughly 10 km. The low - levelled average precipitation potentially was the fruit from ongoing climate change shifting the raining seasons and making precipitation patterns less predictable.

Chloride concentrations in rainfall varied among the communities as well. Samples in the upstream area measured slightly higher concentrations with similar margins almost throughout the whole time. The reason for that remains unknown, not least

since there is no knowledge about factors influencing chloride dispersion such as fertilizer application, emission rates or wind patterns. This tendency continued for chloride concentrations in groundwater. A remarkable increment at the end and after the minor raining season 2023 suggested less water in the wells. The falling groundwater level during that period confirmed this relation. Simultaneously, lower chloride concentrations came along with rising groundwater tables before the end of the major raining season in 2024. Higher chloride concentrations in Mmrobem were even more striking during surface water monitoring. Peaks were in December 2023 and in July 2024, in offset to the highest flowrates of the periods in October 2023 and June 2024. The strong inclining surface flowrates at Kunsu (KSW) from September on were supposedly due to alteration of the river channel by illegal mining activities. The diversion of the watercourse by Galamsey on the Mankran river upstream of Kunsu heavily impacts its discharge. These anthropogenic interferences may have modified the vegetation, slope, contribution area and permeability. The observations from the citizen scientists indicate a relation between chloride concentrations in rain- surface and groundwater and seasonal rain and dry periods. However, the significantly higher chloride levels throughout all water sources at Mmrobem suggest possible local sources of chloride pollution or differences in environmental factors.

Further limitations of this study are the number and type of soil samples used for scaling prevailing characteristics in the watershed. Especially in the downstream area (Kunsu), unexpected hard soil structure with big gravel and stones jeopardized the equipment and resulted in 99 instead of planned 114 samples in the desired depths of 0 – 10 and 30 – 40 cm respectively. Further, those samples distributed not evenly among the whole watershed nor all determined subplots. As a result, there were subsoil data lacks for both core and auger samples in the downstream area. Additionally, collected soil data including 24 infiltration measurements at 9 plots over 120 km^2 (5/km^2) was little compared to ca. 100 infiltration measurements at an experimental site encompassing one community (Ofori et al., 2013). Others conducted 32 soil samples within 60 km^2 (about two per km^2) (Fosu-Mensah et al., 2016) or had data bases built on more than 3,000 plots like in Bargués – Tobella et al., 2024. Therefore, it is suggested that presented values describing bulk density, pH, organic matter and texture are not sufficient for explaining locally variable conditions in the Mankran watershed. They did however give a more detailed idea than global databases with low resolution.

While Infiltration measurements contributed in understanding top soil infiltration processes, the improvised PVC ring infiltrometers designed after the recommendations of Bargués – Tobella et al., 2024 arguably led to outstanding Kfs at the cocoa subplots. Repeated penetration into the soil created small cracks at the

bottom of the devices possibly augmenting water infiltration rates in more porous soils. Since time constraints did not allow unlimited infiltration measurements, the real moment of stabilization potentially remained unknown.

Other weaknesses tied to the applicability of the Chloride Mass Balance and Water Table Fluctuation method respectively. Primarily, the amount of wells collecting the basic data for application of both methods distributed unevenly throughout the watershed. There was one well upstream (Mmrobem), three midstream (Barniekrom) and two downstream (Kunsu) monitoring groundwater levels and chloride concentrations. Averaging multiple wells from the same area balanced outliers and missing data. Thus, groundwater level data at Barniekrom is potentially more robust to those errors than data at the other areas. Further, the rainfall amounts collected by citizen scientists in the upstream area (Mmrobem) were unusually low. Especially during the major raining season in 2024, monitored precipitation was varying substantially up to 300 mm/month within 20 km and among the three communities. Further, high variabilities in estimated Specific yield (S_y) led to recharge numbers exceeding 100 % of the monitored rainfall. Not least since, retrieved FC was far outside comparable data. Commonly used geological data from literature delivered lower S_y values and helped in narrowing down the recharge estimations, especially for the up - and downstream areas. It was only due to those results, that comparison with CMB recharge rates were possible. Such low S_y, however, is contradictory to the characteristic fractures and joints in crystalline rocks dominating the area. This discrepancy exemplifies the complexity in soil and water relations and shows the need for a more robust estimation of S_y using multiple methods.

In addition, as observed by Abera Beyene et al., 2019, spatially far distributed groundwater wells showed highly varying recharge rates. Therefore, averaging an overall recharge representative for the entire area was difficult. The WTF assumes recharge in unconfined aquifers is solely due to rainwater reaching the water table and it is ideal for shallow groundwater with significant level changes. Since simple clamp meters measured the water tables manually, minor daily changes in water table were difficult to detect. However, groundwater level monitoring did not reveal any influences of the mining activities. The shallow water tables in the downstream area (Kunsu) were not fluctuating more than in other wells.

Chloride concentrations in rain – ground – and surface water in the upper watershed (Mmrobem) were higher than those in the middle (Barniekrom). Possible pollution or environmental chloride intake limits the applicability of the CMB. Contaminated samples in July 2023 and March 2024 further aggravated ground water recharge

projection by this method. Additionally, surface runoff calculated with a flowrate of a leave drop arguably delivered biased data.

A final constraint was the amount of time available for analysing collected soil data. More advanced statistical approaches could have tested on inter factorial interaction among landscape position, land use and depth, possibly connecting soil conditions further with groundwater recharge estimations. Nevertheless, learning how to handle those statistical packages would have demanded more time.

4.3 Contributions and recommendations for future research

The climatic and vegetation spectrum of the Mankran watershed was the least comprehensive in the data compilation of Bargués - Tobella et al., 2024. Besides estimating potential groundwater recharge, this study contributed in improving knowledge of soil physical properties in humid environments and especially forest cocoa dominated landscape. Data below 30 cm as well as infiltration measurements in cocoa fields, further brought novelty. The observed spatial variability in soil texture, bulk density, and infiltration rates underscores the need for management practices to optimize water resources and improve soil health. The attempt to show importance of examined soil physical properties for understanding of groundwater recharge patterns was insufficient. Recharge favouring conditions only partly supported actual recharge estimations. Soil physical properties and fastest infiltration rates at cocoa forest dominated upstream (Mmrobem) did not deliver the highest groundwater recharge. Instead, the downstream section (Kunsu) exceeded WTF projections for Mmrobem and Barniekrom marginally. Higher clay fractions in Barniekrom did not mirror in lower groundwater recharge projections for this area. Thereby, discrepancy with soil properties remains highlighting the complex interplay between land use, soil characteristics and groundwater recharge. Enhancing soil structure in agricultural areas could, however, improve water infiltration and reduce runoff while simultaneously mitigating flood risk and promoting sustainable groundwater recharge.

Future research should set focus on long-term monitoring of groundwater levels and recharge rates including multiple hydrological years. State of the art pressure plate analysis and methods involving costly but reliable pumping tests could not only deliver more robust S_y measurements but upgrade the application of the WTF method. Expanded soil sampling in lower depths as well as better knowledge of spatial tree cover and therefore ongoing evapotranspiration processes would further help in understanding deep percolation and groundwater recharge. Including more

comprehensive rainfall and runoff data could strengthen the CMB approach. Further exploration of impacts by land use changes on soil properties and hydrological processes will be crucial for developing adaptive management strategies in the face of climate variability and increasing anthropogenic pressures. The citizen scientists approach could be a useful tool for pursuing these paths.

5. CONCLUSION

This study assessed soil characteristics and groundwater recharge in the Mankran watershed. Soil physical properties partially varying with land use, depth and geographic position provided different conditions for infiltration and percolation of rainwater. The results further highlighted the complexity of groundwater recharge processes in humid environments and the need for multiple estimation methods to capture variability accurately.

Both applied methods, CMB and WTF, delivered valuable insights but revealed often strongly differing recharge rates with CMB being more conservative. From 16th June 2023 – 31st July 2024, they projected groundwater recharge downstream (Kunsu) with 56 % (672 mm), the more clayish midstream (Barniekrom) at 17 – 44 % (204 – 528 mm) and sandier upstream (Mmrobem) averaging 12 % (144 mm) although having more promising soil conditions. Generally, local soil data pointed out recharge favouring conditions, which did not always support estimations by WTF and CMB. Further, Specific Yield (S_y) proofed to be a very sensible term decisively defining results by WTF. Thus, the need for more comprehensive sampling and monitoring to enhance the reliability of local soil data and consequently S_y is evident. Future research should focus on increasing the density of soil sampling, especially in the deeper soil layers. Refined estimation methods could further improve the accuracy of groundwater recharge assessments.

References

AASWDA. (2018). Ahafo Ano South-West District Assembly; District Medium-Term Development Plan (2018-2021) Under The Medium-Term National Development Policy Framework: "An Agenda For Jobs: Creating Prosperity And Equal Opportunity For All (2018-2021)."

Abbott, T. S. (1987). Soil testing service: Methods and interpretation/Biological and Chemical Research Institute. Department of Agriculture, New South Wales; Biological and Chemical Research Institute (N.S.W.). https://catalogue.nla.gov.au/catalog/287528

Abera Beyene, A., Verhoest, N. E. C., Tilahun, S., Alamirew, T., Adgo, E., & Nyssen, J. (2019). Irrigation efficiency and shallow groundwater in anisotropic floodplain soils near Lake Tana, Ethiopia. Irrigation and Drainage, 68(2), 365–378. https://doi.org/10.1002/ird.2320

Addisie, M. B. (2022). Groundwater recharge estimation using water table fluctuation and empirical methods. H2Open Journal, 5(3), 457–468. https://doi.org/10.2166/h2oj.2022.026

Adu, S. V. (1992). Soils of the Kumasi Region of Ghana. Soil Research Institute.

Adusei-Gyamfi, J., Gyebi, A. S. A., Amponsah, A. K., Atampugre, G., Tilahun, S. A., & Cofie, O. (2023). Evaluating hydrological dynamics and water quality in agricultural landscapes in Ghana's Forest Transition Belt: A citizen science approach. Colombo, Sri Lanka: International Water Management Institute (IWMI). CGIAR Initiative on West and Central African Food Systems Transformation. 38p.

Agyei Duodu, J. (2009). Geological map of Ghana 1:1 000 000. Geological Survey Department ; Bundesanstalt für Geowissenschaften und Rohstoffe.

Akurugu, B., Chegbeleh, L. P., & Yidana, S. (2019). Characterisation of groundwater flow and recharge in crystalline basement rocks in the Talensi District, Northern Ghana. Journal of African Earth Sciences, 161, 103665. https://doi.org/10.1016/j.jafrearsci.2019.103665

Allison, G. B., Gee, G. W., & Tyler, S. W. (1994). Vadose-Zone Techniques for Estimating Groundwater Recharge in Arid and Semiarid Regions. Soil Science Society of America Journal, 58(1), 6–14. https://doi.org/10.2136/sssaj1994.03615995005800010002x

Anim-Gyampo, Ing. Prof. M., Berdie, B., Bessah, E., & Agodzo, S. (2021). Effects of Illegal Artisanal Gold Mining Operations on Groundwater Quality in Ghana: The Case of Ahafo-Ano South District (pp. 1–16). https://doi.org/10.5772/intechopen.100242

Appiah-Adjei, E. K., & Osei-Nuamah, I. (2017). Hydrogeological evaluation of geological formations in Ashanti Region, Ghana. Journal of Science and Technology (Ghana), 37(1), Article 1. https://doi.org/10.4314/just.v37i1.4

Asomaning, G. (1992). Groundwater resources of the Birim basin in Ghana. Journal of African Earth Sciences (and the Middle East), 15(3), 375–384. https://doi.org/10.1016/0899-5362(92)90022-5

Assefa, T. T., Atampugre, G., Tilahun, S., & Cofie, O. (2023). Modeling of water availability for food system transformation in Upper Offin Sub-basin and Mankran Micro-watershed of Ghana: A baseline study. https://hdl.handle.net/10568/139354

Austin, R., Gatiboni, L., & Havlin, J. (2020). Soil Sampling Strategies for Site-Specific Field Management | NC State Extension Publications. https://content.ces.ncsu.edu/soil-sampling-strategies-for-site-specific-field-management

Baffour, N. K., Atakora, E., Ofori, E., & Antwi, B. O. (2012). Estimation of soil erodibility and rainfall erosivity for the biemso basin, Ghana. Journal of Environmental Hydrology, 20.

Bargués-Tobella, A., Winowiecki, L. A., Sheil, D., & Vågen, T.-G. (2024). Determinants of Soil Field-Saturated Hydraulic Conductivity Across Sub-Saharan Africa: Texture and Beyond. Water Resources Research, 60(1), e2023WR035510. https://doi.org/10.1029/2023WR035510

Bationo, A., Ngaradoum, D., Youl, S., Lompo, F., & Fening, J. O. (Eds.). (2018). Improving the Profitability, Sustainability and Efficiency of Nutrients Through Site Specific Fertilizer Recommendations in West Africa Agro-Ecosystems: Volume 2. Springer International Publishing. https://doi.org/10.1007/978-3-319-58792-9

Bazuhair, A. S., & Wood, W. W. (1996). Chloride mass-balance method for estimating ground water recharge in arid areas: Examples from western Saudi Arabia. Journal of Hydrology, 186(1), 153–159. https://doi.org/10.1016/S0022-1694(96)03028-4

Boansi Okofo, L., Adonadaga, M.-G., & Martienssen, M. (2022). Groundwater age dating using multi-environmental tracers (SF6, CFC-11, CFC-12, δ18O, and δD) to investigate groundwater residence times and recharge processes in Northeastern Ghana. Journal of Hydrology, 610, 127821. https://doi.org/10.1016/j.jhydrol.2022.127821

Choi, I.-H., Woo, N., Kim, S.-J., Moon, S.-K., & Kim, J. (2007). Estimation of the Groundwater Recharge Rate during a Rainy Season at a Headwater Catchment in Gwangneung, Korea. Korean Journal of Agricultural and Forest Meteorology, 9, 75–87. https://doi.org/10.5532/KJAFM.2007.9.2.075

Christiansen, E., & Awadzi, T. W. (2000). Water balance in a moist semi-deciduous forest in Ghana. West African Journal of Applied Ecology, 1(1), Article 1. https://doi.org/10.4314/wajae.v1i1.40566

Dapaah-Siakwan, S., & Gyau-Boakye, P. (2000). Hydrogeologic framework and borehole yields in Ghana. Hydrogeology Journal, 8, 405–416. https://doi.org/10.1007/PL00010976

Dekongmen, B. W., Anornu, G. K., Kabo-Bah, A. T., Larbi, I., Sunkari, E. D., Dile, Y. T., Agyare, A., & Gyamfi, C. (2022). Groundwater recharge estimation and potential recharge mapping in the Afram Plains of Ghana using SWAT and remote sensing techniques. Groundwater for Sustainable Development, 17, 100741. https://doi.org/10.1016/j.gsd.2022.100741

Delin, G. N., Healy, R. W., Lorenz, D. L., & Nimmo, J. R. (2007). Comparison of local- to regional-scale estimates of ground-water recharge in Minnesota, USA. Journal of Hydrology, 334(1), 231–249. https://doi.org/10.1016/j.jhydrol.2006.10.010

Dinkins, C. P., & Jones, C. (2008). Soil Sampling Strategies.

Driessen, P., Deckers, J., Spaargaren, O., & Nachtergaele, F. (2001). Lecture notes on the major soils of the world. Food and Agriculture Organization of the United Nations (FAO). https://research.utwente.nl/en/publications/lecture-notes-on-the-major-soils-of-the-world

Duah, A. A., Akurugu, B. A., Darko, P. K., Manu, E., & Mainoo, P. A. (2021). Groundwater recharge and potential exploitation in the Densu basin, Southwestern Ghana. Journal of African Earth Sciences, 183, 104332. https://doi.org/10.1016/j.jafrearsci.2021.104332

Effland, W. R., Asiamah, R. D., Adjei-Gyapong, T., Dela-Dedzoe, C., & Boateng, E. (2009). Discovering Soils in the Tropics: Soil Classification in Ghana. Soil Horizons, 50. https://doi.org/10.2136/sh2009.2.0039

Enahoro, D., Mensah, C., & Sika, G. (2023). What do we know about the future of food, land and water systems in West and Central Africa? https://www.cgiar.org/news-events/news/what-do-we-know-about-the-future-of-food-land-and-water-systems-in-west-and-central-africa/

FAO. (2022). Food and Agriculture Organization of the United Nations. FAOSTAT Statistical Database. https://www.fao.org/faostat/en/#data.

Farrick, K. K., & Gittens, D. (2023). Infiltration and soil water repellency in plantations: Stand and seasonal effects. Ecohydrology, 16(2), e2499. https://doi.org/10.1002/eco.2499

Fosu-Mensah, B., Okoffo, E., Darko, G., & Gordon, C. (2016). Assessment of organochlorine pesticide residues in soils and drinking water sources from cocoa farms in Ghana. SpringerPlus, 5, 19. https://doi.org/10.1186/s40064-016-2352-9

Gibrilla, A., Fianko, J. R., Ganyaglo, S., Adomako, D., Stigter, T. Y., Salifu, M., Anornu, G., Zango, M. S., & Zakaria, N. (2022). Understanding recharge mechanisms and surface water contribution to groundwater in granitic aquifers, Ghana: Insights from stable isotopes of δ2H and δ18O. Journal of African Earth Sciences, 192, 104567. https://doi.org/10.1016/j.jafrearsci.2022.104567

Gill, H. E. (1969). A ground-water reconnaissance of the Republic of Ghana, with a description of geohydrologic provinces. In Water Supply Paper (1757-K). U.S. Govt. Print. Off.,. https://doi.org/10.3133/wsp1757K

Guan, H., A, L., Simmons, C., Z, D., & J, H. (2009). Catchment conceptualisation for examining applicability of chloride mass balance method in an area of historical forest clearance. Hydrology and Earth System Sciences Discussions, 6. https://doi.org/10.5194/hessd-6-7025-2009

Gupta, S., Hengl, T., Lehmann, P., Bonetti, S., & Or, D. (2021). SoilKsatDB: Global database of soil saturated hydraulic conductivity measurements for geoscience applications. Earth System Science Data, 13(4), 1593–1612. https://doi.org/10.5194/essd-13-1593-2021

Hastenrath, S. (1985). Climate and circulation of the tropics. Springer Netherlands. https://doi.org/10.1007/978-94-009-5388-8

Healy, R. W. (2010). Estimating Groundwater Recharge. Cambridge University Press. https://doi.org/10.1017/CBO9780511780745

Healy, R. W., & Cook, P. G. (2002). Using groundwater levels to estimate recharge. Hydrogeology Journal, 10(1), 91–109. https://doi.org/10.1007/s10040-001-0178-0

ICARDA. (2024). Water Balance- Theoretical Basis – Regional Water Harvesting Potential Mapping Project. http://mena-rainwater.org/water-balance/

Johnson, A. I. (1967). Specific yield: Compilation of specific yields for various materials. In Water Supply Paper (1662-D). U.S. Government Printing Office. https://doi.org/10.3133/wsp1662D

Kesse, G. O. (1985). The mineral and rock resources of Ghana. https://www.osti.gov/biblio/6752942

Loheide II, S. P., Butler Jr., J. J., & Gorelick, S. M. (2005). Estimation of groundwater consumption by phreatophytes using diurnal water table fluctuations: A saturated-unsaturated flow assessment. Water Resources Research, 41(7). https://doi.org/10.1029/2005WR003942

Lutz, A., Minyila, S., Saga, B., Diarra, S., Apambire, B., & Thomas, J. (2015). Fluctuation of Groundwater Levels and Recharge Patterns in Northern Ghana. Climate, 3(1), Article 1. https://doi.org/10.3390/cli3010001

Lv, M., Xu, Z., Yang, Z.-L., Lu, H., & Lv, M. (2021). A Comprehensive Review of Specific Yield in Land Surface and Groundwater Studies. Journal of Advances in Modeling Earth Systems, 13(2), e2020MS002270. https://doi.org/10.1029/2020MS002270

Manu, E., De Lucia, M., Akiti, T., & Kühn, M. (2023). Stable Isotopes and Water Level Monitoring Integrated to Characterize Groundwater Recharge in the Pra Basin, Ghana. Water, 15, 3760. https://doi.org/10.3390/w15213760

McIntyre, D. S. (1974). Methods of Analysis for Irrigated Soils. (Technical Communication No 54). Commonwealth Agricultural Bureaux.

Meinzer, O. E. (1923). Outline of ground-water hydrology, with definitions. In Water Supply Paper (494). U.S. Govt. Print. Off.,. https://doi.org/10.3133/wsp494

Mensah, A. M. (2009). The influence of land-use activities on nutrient inputs into upland catchment streams, Ghana. Ecology and Development Series No. 67.

Ministry of Food and Agriculture, R. of G. (2024). Ahafo Ano South. District Summary; Ahafo Ano South. https://mofa.gov.gh/site/sports/district-directorates/ashanti-region/145-ahafo-ano-south

Mohammed, A. M., Robinson, J. S., Midmore, D., & Verhoef, A. (2016). Carbon storage in Ghanaian cocoa ecosystems. Carbon Balance and Management, 11(1), 6. https://doi.org/10.1186/s13021-016-0045-x

National Research Council. (1994). Ground Water Recharge Using Waters of Impaired Quality. National Academies Press. https://doi.org/10.17226/4780

Nimmo, J. R., Schmidt, K. M., Perkins, K. S., & Stock, J. D. (2009). Rapid measurement of field-saturated hydraulic conductivity for areal characterization. Vadose Zone Journal, 8(1), 142–149. https://doi.org/10.2136/vzj2007.0159

Obuobie, E., Diekkrueger, B., Agyekum, W., & Agodzo, S. (2012). Groundwater level monitoring and recharge estimation in the White Volta River basin of Ghana. Journal of African Earth Sciences, 71–72, 80–86. https://doi.org/10.1016/j.jafrearsci.2012.06.005

Ofori, E., Atakora, E., Kyei-Baffour, N., & Antwi, B. O. (2013). Relationship between landscape positions and selected soil properties at a Sawah site in Ghana. African Journal of Agricultural Research, 8, 3646–3652. https://doi.org/10.5897/AJAR12.150

Ofosu, B., Akayuli, C., Nyako, S., Opuni, K., & Mensah, F. (2014). GIS based Groundwater Level Mapping in Ashanti Region of Ghana. International Journal of Sciences: Basic and Applied Research (IJSBAR), 13, 129–139.

Okoh, P. A., & Zakpaa, H. D. (2024). Soil analysis of a mined-out area at Afiesa, Ghana. Environmental Technology and Science Journal, 15, 105–112. https://doi.org/10.4314/etsj.v15i1.11

Page, A. L. (1982). Methods of Soil Analysis: Part 2 Chemical and Microbiological Properties. In Methods of Soil Analysis. John Wiley & Sons, Ltd. https://doi.org/10.2134/agronmonogr9.2.2ed.frontmatter

Reynolds, D., Elrick, D., & Youngs, E. (2002). Ring or cylinder infiltrometers (vadose zone). Methods of Soil Analysis, 818–826.

Reynolds, W. D., & Elrick, D. E. (1990). Ponded Infiltration From a Single Ring: I. Analysis of Steady Flow. Soil Science Society of America Journal, 54(5), 1233–1241. https://doi.org/10.2136/sssaj1990.03615995005400050006x

Richey, A. S., Thomas, B. F., Lo, M.-H., Famiglietti, J. S., Swenson, S., & Rodell, M. (2015). Uncertainty in global groundwater storage estimates in a Total Groundwater Stress framework. Water Resources Research, 51(7), 5198–5216. https://doi.org/10.1002/2015WR017351

Rutledge, A. T. (1998). Computer programs for describing the recession of ground-water discharge and for estimating mean ground-water recharge and discharge from streamflow records-update. In Water-Resources Investigations Report (98–4148). U.S. Dept. of the Interior, U.S. Geological Survey ; Information Services,. https://doi.org/10.3133/wri984148

Sami, K., & Hughes, D. A. (1996). A comparison of recharge estimates to a fractured sedimentary aquifer in South Africa from a chloride mass balance and an integrated surface-subsurface model. Journal of Hydrology, 179(1), 111–136. https://doi.org/10.1016/0022-1694(95)02843-9

Scanlon, B. R., Healy, R. W., & Cook, P. G. (2002). Choosing appropriate techniques for quantifying groundwater recharge. Hydrogeology Journal, 10(1), 18–39. https://doi.org/10.1007/s10040-001-0176-2

Somaratne, N., & Smettem, K. (2013). Theory of the generalized chloride mass balance method for recharge estimation in groundwater basins characterised by point and diffuse recharge. Hydrology and Earth System Sciences Discussions, 11. https://doi.org/10.5194/hessd-11-307-2014

Sophocleous, M. A. (1991). Combining the soilwater balance and water-level fluctuation methods to estimate natural groundwater recharge: Practical aspects. Journal of Hydrology, 124(3–4), 229–241.

Sparks, A. H., & Hengl, T. (2017). Soil texture classses (USDA system) for 6 soil depths (0, 10, 30, 60, 100 and 200 cm) at 250 m (v0.2) (Data set). Zenodo. (Version 1.0.0) [Computer software]. Zenodo. https://doi.org/10.5281/zenodo.252817

The World Bank Group. (2021). World Bank Climate Change Knowledge Portal. Climate Change, Country Overview: Ghana. https://climateknowledgeportal.worldbank.org/

Tilahun, S., Amponsah, A. K., Atampugre, G., Zemadim, B., Dembélé, M., Darko, S., Mabhaudhi, T., & Cofie, O. (2023). Integrated Land and Water Resources Assessment for Sustainable Irrigation Development in Changing Agroforestry Landscapes: A Case Study of Ghana. https://doi.org/10.2139/ssrn.4652846

Vågen, T. G., Winowiecki, L., & Tondoh, J. E. (2020). Land Degredation Surveillance Framework (LDSF): Field Guide. https://cgspace.cgiar.org/bitstream/handle/10568/49624/ldsffieldguide2010.pdf?sequence=1

Varni, M., Comas, R., Weinzettel, P., & Dietrich, S. (2013). Application of the water table fluctuation method to characterize groundwater recharge in the Pampa plain, Argentina. Hydrological Sciences Journal, 58(7), 1445–1455. https://doi.org/10.1080/02626667.2013.833663

Walker, D., Parkin, G., Schmitter, P., Gowing, J., Tilahun, S. A., Haile, A. T., & Yimam, A. Y. (2019). Insights From a Multi-Method Recharge Estimation Comparison Study. Groundwater, 57(2), 245–258. https://doi.org/10.1111/gwat.12801

Yidana, S. M., Essel, S. K., Addai, M. O., & Fynn, O. F. (2015). A preliminary analysis of the hydrogeological conditions and groundwater flow in some parts of a crystalline aquifer system: Afigya Sekyere South District, Ghana. Journal of African Earth Sciences, 104, 132–139. https://doi.org/10.1016/j.jafrearsci.2014.12.011

Zango, M. S., Anim-Gyampo, M., Gibrilla, A., Pelig-Ba, K. B., & Okofo, L. B. (2023). Groundwater recharge and dating in crystalline basement aquifers of Vea catchment: An integrated environmental tracers' approach. Scientific African, 19, e01505. https://doi.org/10.1016/j.sciaf.2022.e01505

Popular science summary

The Ashanti region of Ghana experiences changing land use patterns and shifting rainfall trends. These changes affect soil conditions and the ability of rainwater to infiltrate into the ground, a process known as groundwater recharge. Groundwater is a vital resource, especially in tropical regions, as it ensures water availability during dry periods.

This study focuses on understanding how different soil properties influence groundwater recharge in the Mankran watershed, an area dominated by cocoa farms and affected by illegal mining activities. By analysing soil samples from various depths and using two scientific methods, the Chloride Mass Balance (CMB) and Water Table Fluctuation (WTF) methods, the research improves knowledge about the soil characteristics in the area and estimates shallow groundwater recharge.

The findings reveal that soils with high sand content are dominating in the watershed. This favours high infiltration rates, meaning that rainwater can percolate easier into the ground. Less compaction in the topsoil, as in cocoa fields, results in similar effects. The study also shows that groundwater recharge rates vary significantly depending on the method used, with the CMB method indicating seasonal recharge rates of 10 – 34 % of the rainfall, while the WTF method often suggests higher rates.

These results highlight the complexity of groundwater recharge in the region and show the importance of using multiple methods to get accurate estimates. The study also emphasizes the need for comprehensive soil and water data collection to guide sustainable agricultural practices and land use management in the region. By improving our understanding of these processes, we can better protect groundwater resources and support the agricultural livelihoods.

Acknowledgements

This work was carried out under the CGIAR Initiative on West and Central African Food Systems Transformation, which is grateful for the support of CGIAR Trust Fund contributors (www.cgiar.org/funders). Thereby, I want to thank the International Water Management Institute (IWMI) as part of CGIAR and especially my supervisor Seifu Tilahun for accepting my application and supporting me throughout my time in Ghana. I would also like to express my gratitude to Comfort and all the IWMI associates that made me feel welcomed and shared many great moments with me. Further, I want to thank Alex, Shadrak, Mensah, Afia, Gloria, Selina and all the other helpers in the field or lab. Without your commitment, there would not be any field data for this thesis. Lastly, I want to thank my main supervisor Jennie Barron for giving me the opportunity to do my thesis in collaboration with IWMI.

Appendix 1 – Selected lab analysis

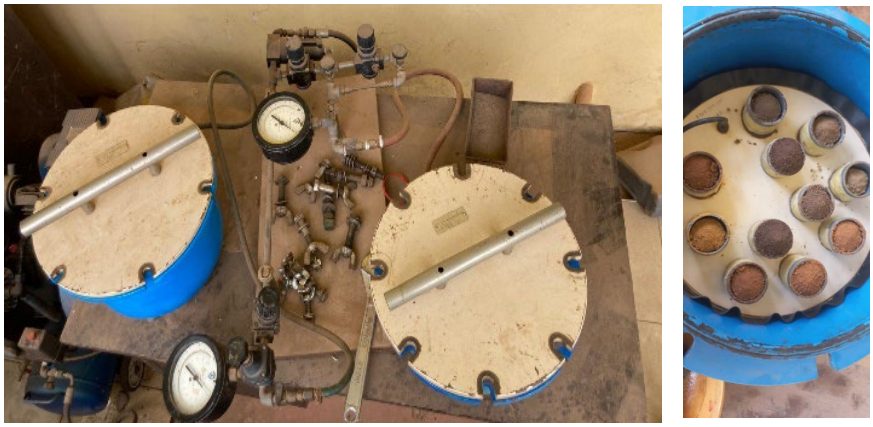

Figure A 1. Pressure plate analysis of loose, disturbed soil samples to retrieve FC and WP

Figure A 2. Hydrometer method for soil texture analysis

Appendix 2 – Collected field data and photos

Figure A 3. From left to right: Dry soil pit with gravel and hard rocks at Kunsu built-up subplot;Clayey soil pit at Barniekrom built-up; Sandy soil pit at Mmrobem built-up subplot

Table A 1. Collected soil data in 0 - 10 and 30 - 40 cm at Kunsu, Barniekrom and Mmrobem

Kunsu	Land use type	B.D(g/cm-3)	Depth (cm)	pH	O.M (%)	SAND (%)	SILT (%)	CLAY (%)	Texture after USDA	FC (%)	WP (%)	Kfs (mm/hour)
KM-up-1	mining	1.40	0-10	5.1	1.10	72.4	7.28	20.32	Sandy clay loam			
KM-up-2	mining	1.38	0-10	5.37	1.31	54.32	9.16	36.52	Sandy clay			
KM-up-3	mining	1.45	0-10	5.38	1.17	74.32	17.2	8.48	Sandy loam			
KP-up-1	plantain	1.15	0-10	6.19	4.88	66.2	9.12	24.68	Sandy clay loam			31.7
KP-up-2	plantain	1.22	0-10	6.71	4.68	86.2	8.96	4.84	Loamy sand			11.4
KP-up-3	plantain	1.16	0-10	6.96	5.50	84.12	9.04	6.84	Loamy sand			49.1
KP-low-1	plantain	1.58	30-40									
KP-low-2	plantain	1.43	30-40									
KP-low-3	plantain	1.55	30-40									
KSY-up 1	built up	1.63	0-10	7.11	1.86	78.2	6.84	14.96	Sandy loam	18.93	10.76	20.2
KSY-up 2	built up	1.57	0-10	7.14	1.03	74.12	8.92	16.96	Sandy loam	18.96	11.38	15.9

KSY-up 3	built up	1.62	0-10	7.22	0.89	74.2	12.96	12.84	Sandy loam			9.8
KSY-low-1	built up		30-40							20.64	11.58	
Barniekrom	**Land use type**	**B.D(g/cm-3)**	**Depth (cm)**	**pH**	**O.M (%)**	**SAND (%)**	**SILT (%)**	**CLAY (%)**	**Texture after USDA**	**FC (%)**	**WP (%)**	**Kfs (mm/hour)**
BC-up-1	cocoa	1.17	0-10	5.54	4.13	64.56	13.64	21.8	Sandy clay loam			118.9
BC-up-2	cocoa	1.38	0-10	4.72	3.71	64.6	7.8	27.6	Sandy clay loam			65.0
BC-up-3	cocoa	1.49	0-10	5.23	4.61	68.56	13.48	17.96	Sandy loam			169.1
BC-low-1	cocoa	1.71	30-40	4.95	1.79	60.6	3.72	35.68	Sandy clay			
BC-low-2	cocoa	1.63	30-40	4.81	1.79	60.6	5.8	33.6	Sandy clay loam			
BC-low-3	cocoa	1.59	30-40	5.06	2.41	64.56	5.32	30.12	Sandy clay loam			
BP-up-1	plantain	1.35	0-10	4.82	3.23	82.56	7.48	9.96	Loamy sand			49.4
BP-up-2	plantain	1.41	0-10	5.18	2.89	84.4	11.44	4.16	Loamy sand			56.4
BP-up-3	plantain	1.57	0-10	5.03	1.10	78.4	13.44	8.16	Loamy sand			60.3

BP-low-1	plantain	1.78	30-40	4.77	0.83	64.4	5.8	29.8	Sandy clay loam			
BP-low-2	plantain	1.71	30-40	4.94	1.38	58.56	7.4	34.04	Sandy clay loam			
BP-low-3	plantain	1.75	30-40	4.7	1.03	72.4	5.28	22.32	Sandy clay loam			
BSY-up-1	built up	1.62	0-10	5.48	0.69	82.4	9.12	8.48	Loamy sand	10.60	7.82	4.7
BSY-up-2	built up	1.72	0-10	5.29	1.17	68.32	5.36	26.32	Sandy clay loam			12.0
BSY-up-3	built up	1.59	0-10	5.15	0.89	64.32	7.28	28.4	Sandy clay loam			28.3
BSY-low-1	built up	1.67	30-40	4.72	1.03	60.32	3.52	36.16	Sandy clay	14.36	11.52	
BSY-low-2	built up	1.73	30-40	4.68	0.76	54.32	7.36	38.32	Sandy clay			
BSY-low-3	built up	1.62	30-40	4.92	0.89	52.4	7.2	40.4	Sandy clay			

Table A 2. Collected soil data in 0 - 10 and 30 - 40 cm at Mmrobem

Mmrobem	Land use type	B.D(g/cm-3)	Depth (cm)	pH	O.M (%)	SAND (%)	SILT (%)	CLAY (%)	Texture after USDA	FC (%)	WP (%)	Kfs (mm/hour)
MC-up-1	cocoa	1.11	0-10	7.25	5.43	82.04	13.2	4.76	Loamy sand			293.8
MC-up-2	cocoa	1.03	0-10	7.26	6.26	77.88	15.08	7.04	Loamy sand			135.8
MC-up-3	cocoa	1.17	0-10	7.42	6.67	88.24	8.64	3.12	Sand			160.0
MC-low-1	cocoa	1.62	0-10									
MC-low-2	cocoa	1.60	30-40	7.28	2.89	62.2	18.76	19.04	Sandy loam			
MC-low-3	cocoa	1.57	30-40	7.17	1.51	73.88	9.08	17.04	Sandy loam			
MP-up-1	plantain	1.79	0-10	7.23	1.58	87.88	5.08	7.04	Loamy sand			34.1
MP-up-2	plantain	1.69	0-10	7.01	1.38	89.96	3.16	6.88	Sand			61.8
MP-up-3	plantain	1.82	0-10	7.32	1.51	93.96	1.16	4.88	Sand			49.6
MP-low-1	plantain	1.82	30-40	6.96	0.34	80.04	8.92	11.04	Sandy loam			

MP-low-2	plantain	1.77	30-40	7.28	1.17	79.88	9.16	10.96	Sandy loam			
MP-low-3	plantain	1.73	30-40	7.12	1.58	77.88	11.24	10.88	Sandy loam			
MSY-up-1	built up	1.68	0-10	7.04	1.44	89.88	3.24	6.88	Sand	17.64	10.20	23.4
MSY-up-2	built up	1.73	0-10	7.3	0.96	83.96	7.08	8.96	Loamy sand			68.8
MSY-up-3	built up	1.72	0-10	6.98	1.99	75.84	11.28	12.88	Sandy loam			26.1
MSY-low-1	built up	1.65	30-40	7.1	0.89	57.96	15.16	26.88	Sandy clay loam	18.37	12.10	
MSY-low-2	built up	1.67	30-40	7.32	0.83	63.84	11.28	24.88	Sandy clay loam	13.14	8.17	
MSY-low-3	built up	1.70	30-40	7.23	1.17	83.84	5.28	10.88	Loamy sand			

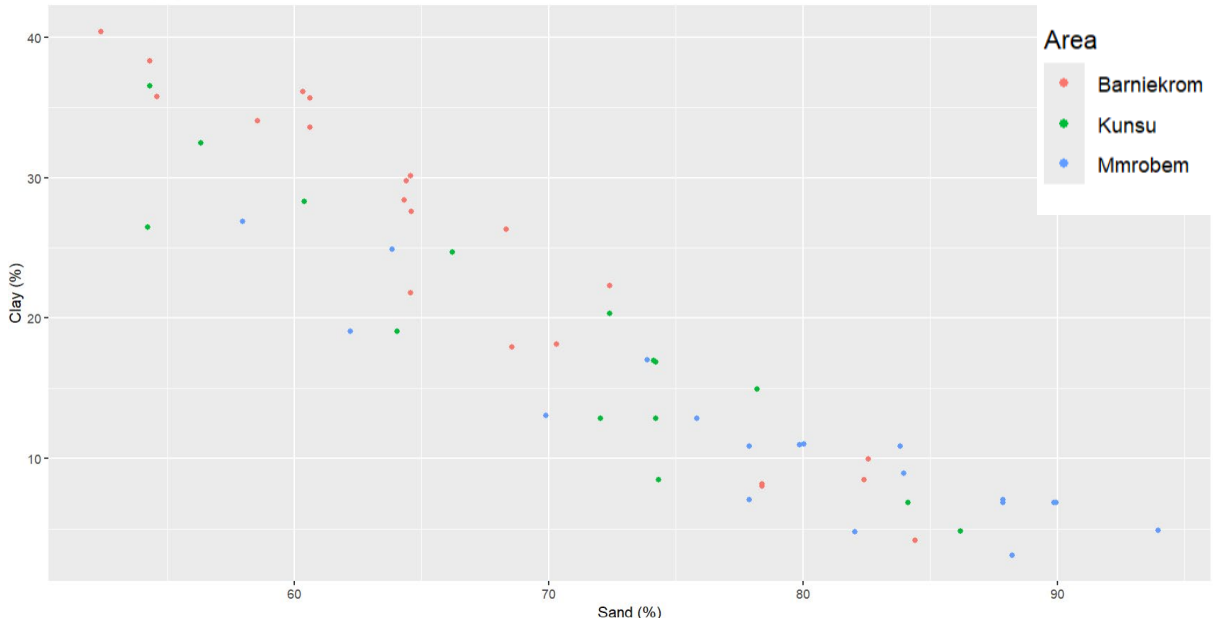

Figure A 4. Scatterplot showing areal relation between clay and sand from collected soil samples

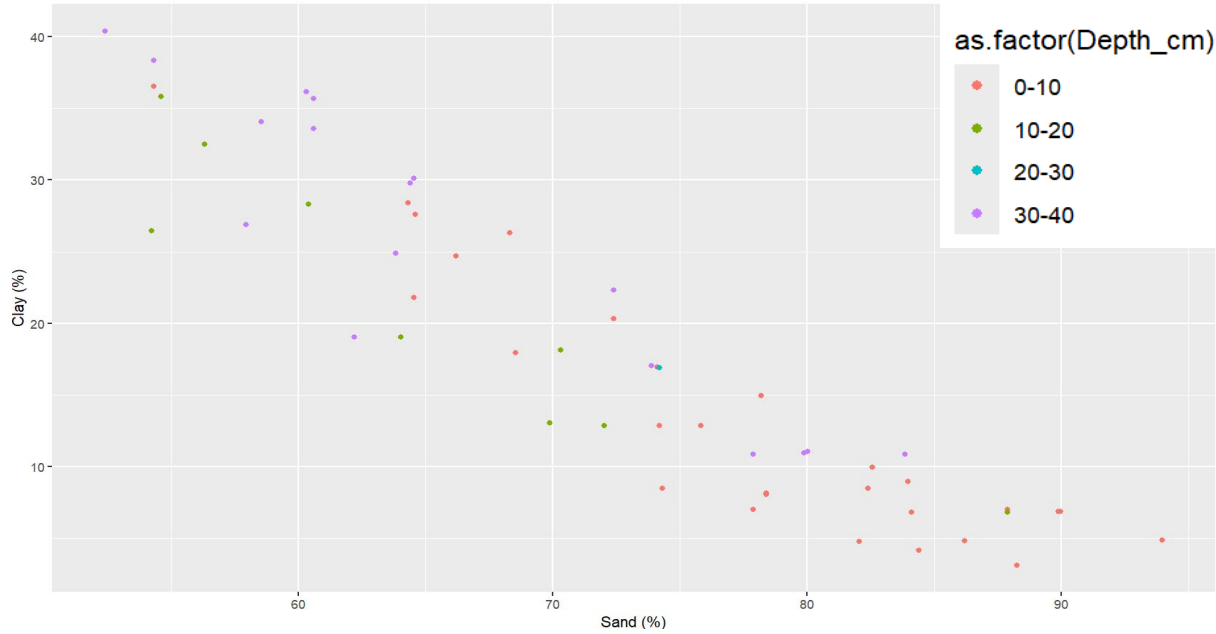

Figure A 5. Scatterplot showing relation between clay and sand from collected soil samples according to depth

Appendix 3 - Groundwater recharge from Water Table Fluctuation method (WTF)

Table A 3. All estimations by Water Table Fluctuation method (including over 100% of precipitation)

Location	16th of June – 31st of November 2023					1st of March – 31st of July 2024				
	Recharge in % of rainfall according to different Sy values									
	Rainfall in mm	Mechanical Analysis	Particle Size Analysis	Reverse Educing Method	Geology	Rainfall in mm	Mechanical Analysis	Particle Size Analysis	Reverse Educing Method	Geology
Kunsu	868	104	160	118	21	524	175	268	198	35
Barniekrom	713	44	18	14	8	832	47	19	15	9
Mmrobem	489	104	150	111	20	189	121	174	129	23
Average all	690	84	109	81	16	515	114	154	114	22

Publishing and archiving

Approved students' theses at SLU are published electronically. As a student, you have the copyright to your own work and need to approve the electronic publishing. If you check the box for **YES**, the full text (pdf file) and metadata will be visible and searchable online. If you check the box for **NO**, only the metadata and the abstract will be visible and searchable online. Nevertheless, when the document is uploaded it will still be archived as a digital file. If you are more than one author, the checked box will be applied to all authors. You will find a link to SLU's publishing agreement here:

- https://libanswers.slu.se/en/faq/228318.

☒ YES, I/we hereby give permission to publish the present thesis in accordance with the SLU agreement regarding the transfer of the right to publish a work.

☐ NO, I/we do not give permission to publish the present work. The work will still be archived and its metadata and abstract will be visible and searchable